RNA metabolism in mycobacteria:
The role of RNase E

Ph.D. Thesis

Ágnes Csanádi M.D.

Department of Medical Microbiology and Immunobiology

University of Szeged

Faculty of Medicine

Szeged

2009

Publications with results incorporated in the thesis

I. Csanadi A, Faludi I, Miczak A. MSMEG_4626 ribonuclease from Mycobacterium smegmatis. *Mol Biol Rep*. 2009**; 36**: 2341-4.   **Impact factor: 1,750**

II. Zeller ME, Csanadi A, Miczak A, Rose T, Bizebard T, Kaberdin VR. Quaternary structure and biochemical properties of mycobacterial RNase E/G. *Biochem J*. 2007; **403**: 207-15.   **Impact factor: 4,009**

III. Kovacs L, Csanadi A, Megyeri K, Kaberdin VR, Miczak A. Mycobacterial RNase E-associated proteins. *Microbiol Immunol*. 2005; **49**: 1003-7. **Impact factor: 1,61**

Introduction

Mycobacteria are very successful pathogens; they are able to survive under adverse conditions. Dynamic regulation of RNA decay and processing should be a very important factor in adapting to environmental changes and disease development. Given the central role of RNase E in RNA processing and decay in *E. coli* and other bacteria, it is conceivable that the RNase E-dependent regulation of RNA stability in mycobacteria might also be a very important mechanism, adjusting the cellular metabolism to environmental changes.

We focus our work on mycobacterial RNase E like proteins. Our results are the first steps towards the understanding of RNA metabolism in mycobacteria and could make finding new drug targets possible.

Pathophysiology

Tuberculosis (TB) has troubled humankind throughout history. It has been a leading cause of death throughout the world, and still is in low- and middle-income countries. TB is a classic example of airborne infection [1]. In nearly all instances, tuberculous infection is acquired by inhalation of one or more tubercle bacilli contained in an airborne particle small enough (1 to 5 μm) to reach an alveolus. Particles that reach the respiratory bronchioles and alveoli are generally ingested by alveolar macrophages and removed from the alveolar space by migration of the phagocytes along the alveolar surface to the origin of the mucociliary transport system [2]. Macrophages, even in individuals with no prior immunologic experience with mycobacterial infection, possess some bacterial-killing or growth-inhibitory capability. Thus, once phagocytosis of a small number of invading mycobacteria is performed by the alveolar macrophages, killing and digestion of the organism probably follow in the majority of exposures to *Mycobacterium tuberculosis*. However, when many droplet nuclei containing tubercle bacilli reach the alveoli, the number of bacilli ingested by an individual macrophage can overwhelm the microbicidal system of the phagocyte. When the nonspecific defences are insufficient to kill all of the organisms, the surviving bacilli multiply, causing a localized tuberculous pneumonia. In general, in the presence of an effective, specific cell-mediated immune response, this lesion heals spontaneously, leaving only a calcified focus (Ghon lesion), which may be accompanied by calcification in hilar nodes, the two lesions together forming the Ranke complex.

During the phase of tissue invasion, transport of organisms through alveolar walls within macrophages provides access to the bloodstream via the lymphatics, and a tuberculous bacillemia ensues [3]. During the course of the bacteraemia, the organisms have access to all organs of the body and tend to persist in sites that provide a favourable environment for growth. It has been postulated that the sites preferred by the organism are those in which the prevailing oxygen tension is the highest. The apical portions of the lungs, the most favoured location of persistence and subsequent proliferation, are known to have a relatively high PO_2, whereas organs such as the heart and spleen have lower levels. Thus, the high frequency of pulmonary involvement (80% to 85% of all cases) as opposed to the near absence of clinical involvement of the heart and spleen is consistent with the interpretation that higher levels of PO_2 favour the growth of the pathogen.

The principal immune response associated with protection against tuberculosis in experimental animals and presumably humans is cell-mediated immunity involving T lymphocytes and macrophages [4]. Studies in *Mycobacterium bovis* bacillus Calmette-Guérin (BCG)-immunized animals indicate that, although immunization does not prevent infection with *M. tuberculosis*, the growth of the organism within macrophages is reduced by several orders of magnitude.[5] In dramatic contrast, immunodeficiency, such as that produced by Human Immunodeficiency Virus (HIV) infection or selective depletion of T cells or cytokines, especially interferon-γ (IFN-γ), in experimental animals, results in a weakening of defences against *M. tuberculosis* [4]. However, because *M. tuberculosis* is a virulent organism, little if any immunodeficiency is necessary for disease development. Thus, TB, which commonly occurs with a lesser degree of immunodeficiency than other HIV-associated infections, has become a sentinel disease for the presence of HIV infection.

Epidemiology

TB is a major threat to global health, recently exacerbated by the emergence of highly drug-resistant forms of the disease-causing pathogen and synergy with HIV / AIDS (Acquired Immunodeficiency Syndrome) [6;7]. A recent report on the TB pandemic revealed that in 2005, there were almost 9 million new cases and 1.6 million deaths [8]. The latest data indicate that the incidence rate has probably stabilized, but the challenge is to reverse the trend and reduce global mortality and, in the long term, to eliminate the disease.

Unfortunately, it has been estimated that one third of the world's population is latently infected with *M. tuberculosis*, providing an enormous reservoir for future disease.

Tuberculosis control

The Stop TB (S TB) Partnership's goal is eliminating TB as a public health problem by 2050. However, the current tools for diagnosing, treating, and preventing TB are inadequate for this task: latent and active TB are most commonly diagnosed using, respectively, a skin test that dates back to 1891 [9] and sputum-smear microscopy from the same era [10]. The current "short-course" drug therapy consists of a cocktail of drugs taken over a period of at least six months, and despite its widespread use, the BCG vaccine is largely ineffective, at least in preventing adult pulmonary disease. A growing problem that has had an impact on the success of treatment programs is the emergence of strains of multidrug-resistant TB (MDR-TB), which is defined as resistance to isoniazid and rifampicin, to the drugs used as first-line treatment. Around 400,000 cases of multidrug- resistant *M. tuberculosis* infection occur per year [11].

Furthermore, essentially untreatable outbreaks of extensively drug-resistant TB (XDR-TB) have begun to appear. XDR-TB is defined as MDR-TB plus resistance to a quinolone and one of the second-line anti-TB injectable drugs (Amikacin, Kanamycin, and Capreomycin).

Directly Observed Therapy "short-course" (DOTS) has conventionally relied on detection of microscopically smear–positive samples and initiation of therapy. In the absence of an effective vaccine, this has been the cornerstone of TB control.

Although DOTS has been very successful at standardizing care practices and increasing cure rates, case-detection targets have been more difficult to achieve [6]. Furthermore, overall TB control, as measured by a decline in incidence, especially in settings where drug resistance or HIV co-infection are prevalent, has been limited [6]. Bacteriological diagnosis of tuberculosis continues to rely on the detection of acid fast bacilli on microscopic examination and on culture. An affordable, rapid diagnostic test that has better sensitivity than smear examination is highly desirable, but remains elusive. Most TB cases will be missed, mostly because of the inherent limits of the sensitivity of the test, which detects only 60% of culture-positive pulmonary TB patients even in clinical trial settings. Moreover, microscopy misses exactly the patients with early disease that would be desirable to detect and treat to block transmission before it has begun. Delays in diagnosis up to 3–6 months are common due to the lack of sensitivity of

microscopical examination [12;13], during this period the disease can progress and cause severe destruction of the airways and continued transmission.

The limitations of the tuberculin skin test (TST) are also well recognised; false positives occur because the purified protein derivative contains many antigens that are present in BCG and non-pathogenic mycobacteria, and false negatives occur in immunocompromised patients, early in primary TB, and in disseminated tuberculosis. 6 kDa early secretory antigenic target (ESAT-6) based and 10 kDa secreted antigen (CFP-10) based enzyme-linked immunospot (ELISpot analysis) is about 90% sensitive for active TB and more specific than the TST in BCG vaccinated individuals and seems less compromised than the TST by the presence of HIV infection[14;15]. Mycobacterial culture is much more sensitive than microscopic examination but requires equipment and training and results are often so slow that they are of little clinical relevance. This has proven especially true in patients with advanced HIV infection, where undetected or improperly treated TB can have a very high mortality, with survival measured in days or weeks [16;17].

The diagnosis of drug resistance by conventional methods takes 6–8 weeks, or even longer if solid media are used and requires laboratory infrastructure, which is so rarely available that only 3% of the 6.5 million TB cases arising annually in high-burden countries of Asia and Africa have access to drug susceptibility testing (DST) [18]. However, microscopic examination of growth in wells that are filled with liquid culture medium, with or without the addition of drugs, enables the rapid (within 10 days) detection of drug resistance [19;20]. Resistance to rifampicin is almost invariably a marker for multidrug resistance, and several techniques are available to detect it rapidly. Sensitivity is lower in clinical specimens [21].

Treatment

Conventional short-course therapy has not changed for decades. The most frequently recommended and effective combination is isoniazid, rifampicin, pyrazinamide, and ethambutol for 2 months, followed by isoniazid and rifampicin for 4 months [22]. This regimen is very effective for treatment of patients with TB, including those with HIV infection [23]. The internationally recommended tuberculosis control strategy is DOTS. An extended version of the strategy, DOTS plus, is used to treat drug-resistant TB. Under programme conditions, completion rates of therapy are variable, partly because many patients discontinue treatment when their symptoms improve. Failure to complete therapy

is associated with longlasting infectious status, relapse, and drug resistance [24]. Unfortunately, acquired rifamycin resistance has arisen in HIV-infected individuals and in those with widespread disease [25]. New antituberculotic drugs are needed to improve the treatment of patients with multidrug-resistant TB, and might enable the duration of treatment to be shortened. Among antimicrobial agents already licensed, some of the newer fluoroquinolones, notably moxifloxacin and gatifloxacin, have good in-vitro activity against *M. tuberculosis*. One concern is that resistance to fluoroquinolones can develop rapidly, especially when these drugs are used as monotherapy to treat suspected bacterial infections of the lower respiratory tract before TB has been diagnosed [26;27]. Moreover, some fluoroquinolones, including gatifloxacin, have been withdrawn postmarketing because of toxic effects. A recently published finding is that meropenem-clavulanate is effective against extensively drug-resistant *M. tuberculosis*. In the study potent activity against laboratory strains of *M. tuberculosis* was observed [minimum inhibitory concentration less than 1 microgram per milliliter], and sterilization of aerobically grown cultures was observed within 14 days. In addition, this combination exhibited inhibitory activity against cultures that mimic the "persistent" state and inhibited the growth of 13 extensively drug-resistant strains of *M. tuberculosis* at the same levels seen for drug-susceptible strains [28].

Treatment of latent tuberculosis infection

Preventive therapy reduces TB incidence in HIV-positive and HIV-negative individuals [29;30]. It is a successful component of tuberculosis control in developed countries. Difficulties in the identification of those at risk, uncertainty about effectiveness in higher-transmission settings, and concerns about cost-effectiveness and acquired drug resistance have limited the implementation of preventive therapy in resource-poor countries. The greatest benefit is in patients who are positive to the skin test. The best-studied regimen is 6–12 months of isoniazid. However, isoniazid resistance can occur if TB arises despite preventive therapy—and is particularly likely to develop when preventive therapy with isoniazid is inadvertently given to patients with subclinical or unrecognised TB. Trials have shown that short courses (2 or 3 months) of rifampicin and pyrazinamide were well tolerated by HIV-positive people, and as effective as standard courses of isoniazid (6 or 12 months) for the prevention of tuberculosis [31]. However, in HIV-negative people it was shown that severe deterioration of liver function occurred 5-10 times more often with rifampicin and pyrazinamide than with isoniazid [32;33]. This

finding shows that data obtained in clinical trials cannot be extrapolated to different populations. Investigators are seeking to understand better the biology of latent infection, with the long-term aim of developing new drugs for latent TB [34;35].

Vaccines

BCG vaccination is still widely used. Consensus exists that BCG provides some protection, especially against severe tuberculosis in children [36]. The duration of protection seems to be variable. BCG does not seem to reduce the transmission of TB, which is a serious shortcoming. A more effective vaccine might greatly improve TB control [37]. Because childhood BCG vaccination has some effectivity, a pragmatic consensus has emerged that novel vaccines should be assessed by the degree of conferred immunity compared to BCG. Considering the success of the natural immune response in controlling most TB infections, it is attractive to propose that a vaccine that can be delivered in advance to exposure and mimics the natural immune response will further reduce the incidence. Running counter to this "classical" vaccine approach is the fact that a major portion of TB cases — particularly the sputum smear–positive cases that contribute most to the further spread of infection — arise from a population of individuals who successfully controlled an initial infection but then failed to mount a protective response against a reinfection or reactivation. In contrast to a typical vaccine-preventable disease, individuals whose immune system has been stimulated by a prior bout of active TB remain highly susceptible to subsequent reinfection [38]. The conventional vaccination model, in which the adaptive immune response learns by repeated stimulation, seems to run backwards in the case of TB.

BCG has variable efficacy against adult forms of TB, showing least effect where it is needed most [39]. This is generally attributed to an inherently weak immunogenicity, to adverse immune-mediated interactions with environmental mycobacteria, and to waning of immune memory [40]. A logical approach to overcoming these problems is to boost BCG by priming an additional pool of mycobacteria-reactive T cells.

Mycobacterium smegmatis vaccine strains expressing foreign antigens are a promising new generation of vaccines that induce remarkably strong and specific immune responses in the mammalian hosts. *M. smegmatis* is a species of rapid growing mycobacteria. It grows fast and can propagate one generation every 1–3 h. It is a non-pathogenic bacterium and a powerful cell immunity adjuvant. *M. smegmatis* has been used as a model system for *M. tuberculosis* and for high-level expression of foreign genes

[41;42;43;44]. Unlike other mycobacterial species, such as BCG, that survive in host cells by inhibiting phagosome maturation, *M. smegmatis* is rapidly destroyed by phagolysosomal proteases in the phagosomes of infected cells [45] and facilitates rapid uptake of expressed antigens in *M. smegmatis* and cross-presentation of them. Recombinant *M. smegmatis* has been tested experimentally as a vaccine candidate for *M. tuberculosis* [46], as an alternative gene expression system to BCG or *M. tuberculosis* [47].

Difficulties of tuberculosis control

Control of HIV-associated tuberculosis

The association between HIV and TB is devastating. The annual incidence of tuberculosis is about 10% in HIV-infected individuals from high-burden communities in both industrialised and developing countries [6]. This risk increases further with serious immunosuppression; an annual incidence as high as 30% has been reported in South African patients with clinically advanced HIV [6]. Not only does HIV infection predispose to the reactivation of latent TB [49], but it is also strongly associated with the transmission of TB between adults in sub-Saharan Africa [50]. High transmission rates of tuberculosis cause large numbers of children to be infected, which is concerning because of rapid disease progression and diagnostic difficulties within this group [51].

Facilities to manage HIV-driven epidemic are restricted, and poor health infrastructure limits their implementation. Antiretroviral treatment has proven to reduce the incidence of TB [48;53;54;55], but the risk of its developing is still much higher than in HIV-negative individuals. Furthermore, the gain in life expectancy is higher during which the patient can contract TB. The detection and cure of active tuberculosis were the most effective interventions [56]. On the other hand co-administration of antiretroviral and antituberculotic therapy is not straightforward for three reasons: interactions between antiretroviral drugs and rifamycins; shared toxicities; and the immune reconstitution inflammatory syndrome [57]. Available data suggest that patients who have been given antiretroviral and antituberculotic therapy are at increased risk of adverse drug reactions [57]. Patients with TB commonly develop the immune reconstitution inflammatory syndrome after starting antiretroviral therapy. This syndrome is characterised by aberrant immunopathological immunity to tuberculosis. TB that was improving under treatment can worsen; non-apparent TB can be unmasked.

Tuberculosis, especially when combined with HIV, remains a formidable problem.

Control of drug resistant tuberculosis

Increase in drug resistance threatens the advances that have been made by wider implementation of rational multidrug therapy through the DOTS strategy. MDR- and XDR-TB are important public health threats that deserve considerable effort, but the root cause of the global problem with drug-resistant pathogens is the armamentarium of slowly acting agents currently used to treat drug-susceptible disease.

Treatment for multidrug-resistant TB is circuitous, less effective, costly, and poorly tolerated. Estimates are that more than 4% of tuberculosis cases worldwide are multidrug resistant, with more than 40% of these patients having been previously treated for TB [24]. Eastern Europe has the highest prevalence: multidrug-resistant TB is found in about 10% and 40% of new and previously treated patients, respectively [24]. In one outbreak of TB in HIV-infected patients, XDR TB cases constituted 24% of all multidrug-resistant cases [58]. As mentioned earlier, this level of resistance makes tuberculosis essentially untreatable. In the study of Gandhi et al. in 85% of patients with XDR tuberculosis, the strain of *M. tuberculosis* had the same genetic background, indicating recent transmission, and 67% had been admitted within the previous 2 years, raising the possibility of nosocomial transmission [58]. This outbreak emphasises the need for new antimycobacterial drugs, increased surveillance and caution in hospitals [59].

Achieving the goals in the S TB plan will require the development of new tools that are substantially better than those available today. This, in turn, will require advance in our knowledge of the disease and the biology of *M. tuberculosis* as well as the application of innovative new approaches and technologies. Much progress has been made in the past decade, and a number of new tools are under development [60;61;62;63;64;65;66]. However, much more needs to be done.

Nevertheless, basic and applied research activity is more intense than ever, and clear progress towards better preventive measures, diagnostic tests, and drug treatment options exists.

Identifying hits can be surprisingly difficult for unusual bacterial enzymes due to a lack of biologically relevant chemical diversity, and because of poorly understood rules for bacterial cell penetration. Even then failure can arise, because it is important to identify not only essential, but also rate-limiting, biochemical transformations.

At the same time diverse conditions exist, where drugs should make an effect. Some lesions contain actively replicating bacilli, whereas others (nodules or consolidations of

various sizes) are still successfully containing their mycobacterial invaders in highly structured collections of immune cells known as granulomas [67]. This heterogeneity of mycobacterial populations means either that a particular target must be vulnerable across all of the physiological states occupied by the bacilli or that the agents in a cocktail used must individually have targets that collectively cover all such states [68]. Lesions containing mycobacteria in nonreplicating states are particularly problematic; as such mycobacteria have an intrinsically low basal metabolism that renders them much less susceptible to conventional mycobactericidal agents.

The importance of RNA metabolism

M. tuberculosis can survive and even replicate in naive macrophages and thus must assimilate carbon and produce energy in the phagosome. *M. tuberculosis* is among the most successful microorganisms that adapt to long-term residence in macrophage phagosomes. Adaptive intracellular gene expression involves genes that are associated with virulence, the general stress response, changes in cell wall structure and alternative-carbon-source utilization pathways and their regulation. The turnover of mRNA plays an important role in the regulation of gene expression [69].

In *E. coli*, a key enzyme of RNA decay is RNase E. It is an essential enzyme, responsible for the initial rate-limiting cleavage in the decay of many mRNAs [reviewed in references 70 and 71], as well as playing an important role in 5S and 16S rRNA processing [72;73;74].

In our laboratory in accordance with other researchers, we believe that RNase E the main enzyme of RNA metabolism is a potential target of drug aiming. In the last decades the importance of RNA regulation became clear and more and more publications appear dedicated to the role of this enzyme in the virulence in human pathogens.

RNase E and the degradosome it organises

RNase E was originally discovered as an RNA processing enzyme [75]. Later it was found that its gene, *rne*, and *ams* (altered messenger stability) are identical [76;77;78], suggesting a key role for RNase E in bacterial RNA processing and decay [79,80]. Subsequent studies revealed that RNase E controls the stability of many [for reviews, see refs. 70 and 81], if not the most, mRNAs in *E. coli* [82] as well as being involved in the processing of tRNA precursors [83] and degradation of small regulatory RNAs [84].

Moreover, RNase E has the ability to affect protein degradation through its role in maturation of the 3' end of tmRNA (SsrA) [85].

Our current knowledge about this enzyme mainly originates from studies of *E. coli* RNase E, which is a site-specific ribonuclease that preferentially cleaves in A/U-rich single-stranded regions of structured RNAs.

E. coli RNase E is indispensable for cell viability [86;87]. Structural data obtained for an N-terminal polypeptide representing the evolutionarily conserved catalytic domain of this protein have revealed the presence of discrete folds with putative functions in RNA recognition and cleavage [88]. Moreover, these data and others [89;90] indicate that the catalytic domain exists as a homotetramer, which has two non-equivalent subunit interfaces organizing the active site of the enzyme. In contrast with the N-terminal catalytic domain, the C-terminal part of *E. coli* RNase E shows very little or no similarity to the equivalent regions of other RNase E homologues [91]. This part of the *E. coli* enzyme contains an extra RNA-binding domain(s) [92;93] and multiple sites for interactions with the 3′ to 5′ phosphorolytic exonuclease PNPase (polynucleotide phosphorylase), the RNA helicase RhlB and the glycolytic enzyme enolase to form the *E. coli* multienzyme complex referred to as 'degradosome' [94;95;96;97]. Interestingly the RNA degradosome proteins comprise parts of the bacterial cytoskeleton [98].

E. coli RNase G [99;72] is encoded by the *rng* gene and was initially termed CafA owing to its effects on the formation of cytoplasmic axial filaments observed upon RNase G overproduction *in vivo* [100;101]. Further studies have revealed that this protein has an endoribonucleolytic activity [102] and is involved in maturation of 16S rRNA *in vivo* [98;72]. Although RNase G functionally overlaps with RNase E and shares 35% identity with and 50% similarity to the N-terminal catalytic part of RNase E [103], this endoribonuclease cannot fully compensate RNase E deficiency in *rne*[ts] mutant strains [86;87].

Owing to their overlapping functions and apparently common origin, RNase E- and RNase G-like proteins are believed to belong to the same family of RNase E/G endoribonucleases that are predicted to exist in many bacteria, including pathogenic species [104;105;106]. Although their biochemical properties and biological functions have not yet been investigated in detail in human pathogens, such studies can offer important insights concerning the role of these endoribonucleases during infection and disease development. Recent results demonstrated the importance of RNase E in bacterial pathogenicity. In yersinia, the RNase E activity impacts the Type Three Secretion System

and plays a general role in infectivity [107]. Magnesium homeostasis is very important for the intracellular survival of salmonella. The Mg^{2+} riboswitch targets the mgtA transcript for the degradation by RNase E when cells are grown in high Mg^{2+} environments [108].

Although the degradation and processing of RNA in *E. coli* is relatively well understood, very little is known about the mechanisms which are involved in RNA metabolism in other species, including mycobacteria. Mycobacteria are very successful pathogens [107], which are able to survive under adverse conditions (long non-replicating persistence, and intracellular survival). Given the central role of RNase E in RNA processing and decay in *E. coli*, it is conceivable that RNase E-dependent regulation of RNA stability in mycobacteria might also represent a very important mechanism adjusting the cellular metabolism to environmental changes. These considerations prompted us to purify and characterize the RNase E/G homologue (MycRne) from the intracellular pathogen *M. tuberculosis*.

The difference between pathogenic and saprophytic mycobacteria on the level of RNA metabolism is not known.

To learn more about RNase E proteins that function in different mycobacterial species, we cloned, overexpressed and purified putative mycobacterial RNase E/G homologues from *M. bovis* BCG (RNase E (Rv2444c) from *M. tuberculosis* H37Rv and MycRne-also referred to as CafA (MT2520) from *M. tuberculosis* CDC1551) and *M. smegmatis* (Srne (MSMEG_4626) from *M. smegmatis* MC2 155) and identified proteins associated with these polypeptides.

We have shown that, similar to *E. coli* RNase G [110] and the catalytic domain of *E. coli* RNase E [89;90], MycRne is a 5′-end-dependent endoribonuclease, which can exist in dimeric and tetrameric forms in solution. Moreover, MycRne can cleave a putative 5S rRNA precursor *in vitro*, and the cleavage occurs very close to the 5′-end of mature 5S rRNA, thus suggesting a role for this endoribonuclease in rRNA processing *in vivo*. Although MycRne and *E. coli* RNase E share some common properties, we have shown in our study that their substrate specificities are only partially overlapping. Taken together, our findings expand the current knowledge about biochemical characteristics of RNase E/G enzymes and provide a basis for further analysis of their putative functions in mycobacteria.

Materials and methods

Bacterial strains and growth conditions

E. coli DH5α, *E. coli* HB101, *E. coli* BL21 (DE3) (Novagen) and *E. coli* BL21-CodonPlus (DE3)-RIL (Stratagene) strains were used. *E. coli* strains were routinely grown in LB (Luria–Bertani) medium supplemented with the appropriate antibiotic(s). *M. bovis* BCG was grown in Middlebrook 7H9 broth or 7H11 agar (Difco) supplemented with 10% Middlebrook OADC (oleic acid/albumin/dextrose/catalase) enrichment (Difco) and 0.05% Tween 80 (Sigma). *M. smegmatis MC2* 155 was grown either in Middlebrook or in LB medium.

Cloning of RNase E from *M. tuberculosis*

A 2.8 kb fragment containing the *rne* gene (Rv2444c) was amplified by PCR, using the oligonucleotide primers myc1 5'-CTG TGC ATA TGA TAG ACG GTG CCC-3' and myc2 5'-CGG AGA TCT GGT CAG TCT AGG CGG-3', with *M. tuberculosis* H37Rv DNA as template [111].

PCR amplification conditions were as recommended by the manufacturer, with a GeneAmpII (Applied Biosystems) thermocycler with Advantage GC cDNA polymerase (BD Biosciences).

The amplified DNA was digested with *Nde*I and *Bgl*II and inserted into p6HisF-11d(*icl*) [112] by digesting it with *Nde*I and *Bam*HI and replacing the *icl* gene.

The resulting plasmid, pMRE1 was used to overexpress RNase E in *E. coli*.

p6HisF11d(*icl*) is a pET-11d (Novagen) based plasmid carrying the 6His and FLAG tags in the N-terminal of the cloned insert.

Cloning of CafA from *M. tuberculosis*

For cloning CafA (gene MT2520), primers myc3 5'-TAA CAT ATG GTG GTG CGC GAC C-3' and myc2 were used with *M. tuberculosis* CDC1551 DNA. The amplified fragment was 1.8 kb. Oligonucleotides were designed by using the complete sequence of the *M. tuberculosis* CDC1551 genomes [113].

The amplified DNA was digested with *Nde*I and *Bgl*II and inserted into p6HisF-11d(*icl*) by digesting it with *Nde*I and *Bam*HI and replacing the *icl* gene.

The resulting plasmid, pMRG1 was used to overexpress CafA in *E. coli*.

Cloning of MSMEG_4626 from *M. smegmatis* MC2 155

A 3.1 kb DNA fragment containing the MSMEG_4626 gene was amplified by PCR, using the following oligonucleotide primers: S1 5'-GTG CAT ATG GCC GAA GAT GCC CAT-3' and S2 5'-ACC GGA TCC GTG ATG CTC GTC TAG-3' and *M. smegmatis* MC2 155 DNA as template. Oligonucleotides were planned using the complete sequence of *M. smegmatis* MC2 155 genome [NCBI Genome Project].

The amplified DNA was digested with *Nde*I and *Bam*HI and inserted into p6HisF-11d(*icl*) by digesting it with the same enzymes and replacing the *icl* gene. The resulting plasmid was pSRNE1.

Expression of the mycobacterial proteins (RNase E, CafA and Srne) in *E. coli*

For overexpression, *E. coli* HB101 (pGP1-4) cells carrying the proper plasmid were grown and treated according to the method of Tabor and Richardson [114]. Briefly, cells containing the plasmids were grown at 32 ^{o}C in LB medium in the presence of the required antibiotics. Overexpression of the protein was induced by raising the temperature to 42 ^{o}C for 20 minutes. After induction, the temperature was reduced to 37 ^{o}C for additional 90 minutes, the cells were harvested by centrifugation and the cell pellets were frozen.

Expression of the mycobacterial proteins (RNase E, CafA) in *M. bovis* BCG

pET plasmids cannot be used in mycobacteria, for this purpose we created new constructs using pMV262 shuttle plasmid [115]. The plasmid pMRE2 carries mycobacterial *rne* with the *csp* promoter (Rv3648c) in pMV262. A 250 bp DNA fragment was amplified by using the primers myc4 5'-AAA TCT AGA TTT GCG GAC CCT TCG T-3'and myc5 5'-GAG ACC ATG GCT CGA TCT TTC CTT-3', and was digested with *Xba*I and *Nco*I and cloned to pMRE1 cut with the same enzymes. The *Xba*I-*Hind*III fragment carrying the *csp* promoter, 6His and FLAG tags and *rne* from pMRE1 was ligated to pMV262 digested with *Xba*I and *Hind*III resulting in the plasmid pMRE2. pMRG2 carries *cafA* in pMV262 and was made by replacing the *rne* gene in pMRE2. These plasmids as well as pMV262(*icl*) coding for isocitrate lyase (Icl) [112] were transformed to *M. bovis* BCG by electroporation. Bacteria were grown to the late logarithmic phase in Middlebrook 7H9 Broth (Difco) with OADC enrichment and 0.05% Tween 80, and the cells were harvested by centrifugation.

Expression of the mycobacterial protein Srne in *M. smegmatis* MC2 155

pSRNE2 was created, which carries MSMEG_4626 after the mycobacterial *icl* promoter (Rv0467), 6His and FLAG tags in pMV262 [115]. I1 5' –ACT ATC TAG ATC CGC AGG ACG TCG A-3' and I2 5'-GAC AGC CAT GGA CAA CTC CTT A-3' primers were used to synthesize the *icl* promoter with *M. tuberculosis* H37Rv chromosomal DNA as template. The amplified DNA was cut with XbaI and NcoI and inserted to pSRNE1 opened with the same enzymes. The *Xba*I – *BamH*I fragment from pSRNE1 was inserted to pMV262, the resulting plasmid is pSRNE2. *M. smegmatis* was transformed with this plasmid by electroporation. Mycobacteria were grown to the late logarithmic phase either in Middlebrook supplemented with 10% Middlebrook OADC enrichment (Difco) or in LB medium.

Purification of RNase E, CafA Srne and Icl

Bacteria were opened in a MiniBeadbeater-8 cell disrupter (BioSpec Products, Inc, Barlesville, Oklahoma), using glass beads (106 µm, Sigma) and adding a protease inhibitor cocktail (Sigma). Proteins RNase E, CafA and Icl were purified from *M. bovis* BCG on an anti-FLAG M2 affinity gel (Sigma), according to the manufacturer's instructions. Ribonuclease E (Srne) was purified from *M. smegmatis* MC2 155 by using Talon Metal Affinity Resin (BD Biosciences) according to the manufacturer's instructions.

Vivaspin 500 centrifugal concentrators (5,000 MWCO) (Vivascience) were used to concentrate the samples. Polyacrylamide gel electrophoresis was carried out according to Laemmli [116].

Identification of protein bands

Gels were stained with Coomassie blue [117]. The gel slices containing the corresponding polypeptides were cut from the gel and analyzed by mass spectrometry (Biological Research Centre, Szeged). Briefly, the proteins were digested with trypsin directly in the gel slices and the resulting products of digestion were eluted and analysed by matrix-assisted laser desorption ionization/time-of-flight mass spectrometry. The resulting peptide mass lists were subjected to a database search. Post source decay analysis was used to confirm the MALDI-TOF results.

Homology search, calculation of the protein parameters.

Homology search was carried out with the computer programs of Altschul *et al.*
[118]. Protein parameters were calculated by the ExPASY Server [119].

Purification of Rne498

E. coli BL21(DE3) strain (Novagen) carrying a pET16b-based plasmid that encodes
the first 498 amino acids of *E. coli* RNase E (Rne498), a C-terminally truncated form of
E. coli RNase E representing its catalytic domain [93] was used to overexpress 6His-
tagged Rne498, and the overexpressed protein was purified using immobilized metal-
affinity chromatography as described previously [93]. The eluate fractions, in which the
purity of Rne498 was greater than 95%, were pooled, dialysed against SB buffer [50 mM
Tris/HCl, pH 8.0, 0.1 mM EDTA, 0.5 M NaCl, 20% (v/v) glycerol and 1 mM DTT
(dithiothreitol)] and stored in small (50 µl) aliquots at −80 °C.

Purification of *M. tuberculosis* RNase E/G for biochemical characterisation

The pMRG1construct, verified by sequencing was used for biochemical
characterisation and transformed into the *E. coli* strain BL21-CodonPlus (DE3)-RIL
(Stratagene).

E. coli cells containing pMRG1 plasmid were grown at 37°C in LB medium
supplemented with ampicillin (100 µg/ml), chloramphenicol (34 µg/ml) and glucose
(0.75%). At an attenuance (D_{600}) of ~0.5, the cell culture was pre-cooled on ice for
45 min, and protein expression was induced by addition of IPTG (isopropyl β-D-
thiogalactoside) to 1 mM and incubated for a further 16 h at 15 °C. Cells were harvested
by centrifugation at 7000 *g* for 15 min, frozen at −20 °C, thawed and suspended in ice-
cold binding buffer (0.5 M NaCl and 20 mM sodium phosphate, pH 7.4) supplemented
with pepstatin (1 µg/ml) and protease inhibitor cocktail (one tablet per 3 g of wet cells)
(Roche). The cells were disrupted by sonication in a Cell Disruptor W375 (Heat Systems
Ultrasonics), the cell lysate was cleared further by centrifugation at 16000 *g* for 15 min at
4 °C, and the supernatant was applied to a HisTrap HP (Amersham Biosciences) column
to purify 6His-tagged MycRne according to the manufacturer's instructions. Column
fractions containing MycRne were combined, supplemented with EDTA and DTT to final
concentrations of 0.1 mM and 1 mM respectively, dialysed extensively against EB buffer
(50 mM NaCl, 20 mM Hepes, pH 7.5, 1 mM DTT and 0.1 mM EDTA) and stored in
small (50 µl) aliquots at −80 °C.

In vitro transcription and labelling of 9S RNA

A DNA fragment including the putative *M. bovis* BCG 9S RNA sequence was PCR-amplified from genomic DNA using primers 9Sfor (5′-TGCTAACCGGCCGAAAACTTA-3′) and 9Srev (5′-AACATACAAAAACACCACCGT-3′), and cloned into the pGEM®-T Easy vector (Promega) at the T cloning site. The resulting plasmid (pMt9S) was verified by sequencing, linearized by *Pst*I (Fermentas), blunted with Klenow enzyme (Fermentas), purified in a 1% agarose gel and used to transcribe 9S RNA with a MEGAscript® T7 kit (Ambion). 9S RNA was purified from a 6% polyacrylamide/urea gel, dephosphorylated with bacterial alkaline phosphatase (Fermentas) and 5′-labelled using T4 polynucleotide phosphorylase (Fermentas) and an excess of [γ-^{32}P]ATP (Amersham Biosciences). 5′-end-labelled 9S RNA was purified from a 6% (w/v) polyacrylamide sequencing gel as described previously [120] and subsequently used for cleavage assays.

Primer extension

Total RNA from *M. bovis* BCG was extracted using the hot phenol method [121]. The 5′-^{32}P-labelled 5S rRNA-specific oligonucleotide 5SPEM (5′-CAGTATCATCGGCGCTGGC-3′) and total RNA (150 ng) were co-precipitated with ethanol, the pellet was air-dried and suspended in 5 μl of annealing buffer (75 mM KCl and 67 mM Tris/HCl, pH 8.3), heated to 70°C, quenched on ice, mixed with 5 μl of RT buffer (75 mM Tris/HCl, pH 8.3, 20 mM MgCl$_2$, 4 mM DTT and 0.8 mM each dNTP) containing 4 units of AMV (avian myeloblastosis virus) reverse transcriptase (Promega) and incubated for 30 min at 42 °C. The reaction was stopped by adding 10 μl of sequencing dye. The sample was denatured at 95 °C for 3 min and analysed on an 8% sequencing gel along with a concurrently run sequencing ladder. The latter was prepared using PstI-digested pMt9S, the same 5′-^{32}P-labelled primer and a Reader™ DNA sequencing kit (Fermentas).

Synthetic oligonucleotide substrates

Ribo-oligonucleotides 5′-ACAGUAUUUG-3′ (BR10), 5′-ACAGAAUUUG-3′ (9SA), 5′-GAAGGAUUUAA-3′ (OmpC), 5′-AAAAAAAAAAAAAAAAAAAAAAAAAAA-3′ (A27), 5′-UUUUUUUUUUUUUUUUUUUUUUUUUUU-3′ (U27),

5′-UUUUUUUUUUUUUGUUUUUUUUUUUUU-3′ (U27G),

5′-UUUUUUUUUUUUUAUUUUUUUUUUUUU-3′ (U27A) and

5′-UUUUUUUUUUUUUCUUUUUUUUUUUUU-3′ (U27C), as well as oligonucleotides

5′-pGGGACAGUAUUUG-3′ (pBR13-Fluor) and 5′-HOGGGACAGUAUUUG-3′

(HO-BR13-Fluor) with a fluorescein tag at their 3′ ends, were purchased from VBC

Genomics, whereas 5′-UUUUUUUUUUUUUXUUUUUUUUUUUUU-3′ (U27ab)

containing an abasic residue (X) was purchased from Dharmacon.

RNase E/G cleavage of oligonucleotide substrates and 9S RNA

RNase E/G cleavage reactions were performed as described previously [120] using

Rne498 or MycRne and 5′-labelled substrates. Ladders (1 nt) were prepared either by

partial alkaline hydrolysis of each 5′-end-labelled substrate in 1 mM EDTA and 50 mM

sodium carbonate, pH 9.2, at 85°C for 20 min, or by partial digestion of 5′-end-labelled

oligonucleotides with S1 nuclease in buffer provided by the manufacturer (Fermentas).

RNase T_1 digests of 9S RNA were prepared by incubation of 5′-end-labelled 9S RNA in

10 mM Tris/HCl, pH 8.0, 100 mM NaCl and 5 mM $MgCl_2$ with RNase T_1 (Fermentas) at

37 °C.

Results

Expression of RNase E from *M. tuberculosis*

RNase E from *M. tuberculosis* H37Rv is a large enzyme consisting of 953 amino acids (GenBank accession no. Rv2444c). Its calculated molecular mass is 103 kDa, but in SDS polyacrylamide gels it migrates as a 150 kDa protein (Fig. 1), thus resembling its *E. coli* homologue. The latter likewise had an aberrant mobility (118 kDa versus 180 kDa), which was explained by the specific amino acid composition of the protein [77]. Our homology search, which was carried out with the computer programs of Pearson and Lipman [122] revealed that *M. tuberculosis* H37Rv RNase E displays 100% identity with the full-length *M. bovis* BCG RNase E.

Expression of *M. smegmatis* Srne

M. smegmatis MSMEG_4626 was cloned and expressed in *E. coli* and *M. smegmatis*. The MSMEG_4626 gene product (Srne) is a large protein consisting of 1037 amino acids. Its calculated molecular weight is 112.7 kDa; because of the 6His and FLAG tags, our fusion protein is 4 kDa larger. In SDS-polyacrylamide gels, it migrates as a 180 kDa protein (Fig. 2).

Associated proteins to RNase E from *M. tuberculosis*

To learn more about the nature of copurifying proteins, we overexpressed *M. tuberculosis* H37Rv RNase E in different bacterial hosts and affinity-purified the corresponding RNase E complexes. Following the purification, preparations of RNase E were analyzed on SDS polyacrylamide gel (Fig. 1) and the copurified proteins were identified by mass spectrometry. Despite the use of protease inhibitors, in addition to the full-length polypeptide (RNase E), the mycobacterial preparation from *E. coli* also contained its proteolytic forms (polypeptides 1, 2 and 6). Band 3 was identified as DnaK. This polypeptide was previously found in the preparations when *E. coli* RNase E was overexpressed upon temperature-induced induction [96]. DnaK is involved in many cellular activities, including the heat shock response. It was not found in the RNase E complex, when RNase E was isolated without overexpression [97]. In a DnaK(-) background, in an experiment, where the role of molecular chaperones in inclusion body formation was studied, the amount of inclusion body protein was 2.5-fold higher, than in

the wild-type strain [123]. Band 5 is lipoamide dehydrogenase (NADH), a component of 2-oxodehydrogenase and pyruvate complexes. Band 8 is a mixture of ribosomal proteins L1 (B3984) and S2 (B0169).

In the RNase E preparation isolated from *M. bovis* BCG (Fig. 1), GroEL (band 4) was identified. This is a chaperonin mediating protein folding and assembly [124]. Bands 7 and 9 are the products of genes Mb1721 and Mb0825c, respectively. These proteins were found in the database as hypothetical proteins. Mb1721 is equivalent to Rv1695 (100 % identity) from *M. tuberculosis* H37Rv. Gene MT1734 from *M. tuberculosis* CDC1551 codes for the same protein. This protein is an inorganic polyphosphate/ATP-NAD kinase (Ppnk). Rv1695 has been cloned and expressed in *E. coli* [125]. Ppnk catalyzes the reaction leading to the formation of NADP by the use of ATP or inorganic polyphosphate, playing a crucial role in the regulation of NAD/NADP level and in biosynthetic reactions in the cell. Its association with RNase E may play a regulatory role by helping to adapt to environmental changes. Mb0825c is equivalent to Rv0802c and MT0822 from *M. tuberculosis* H37Rv and CDC1551, respectively. The protein displays partial similarity with many acetyltransferases and hypothetical proteins. Table I lists the identified proteins and the comparison of the RNase E associated proteins from different bacteria.
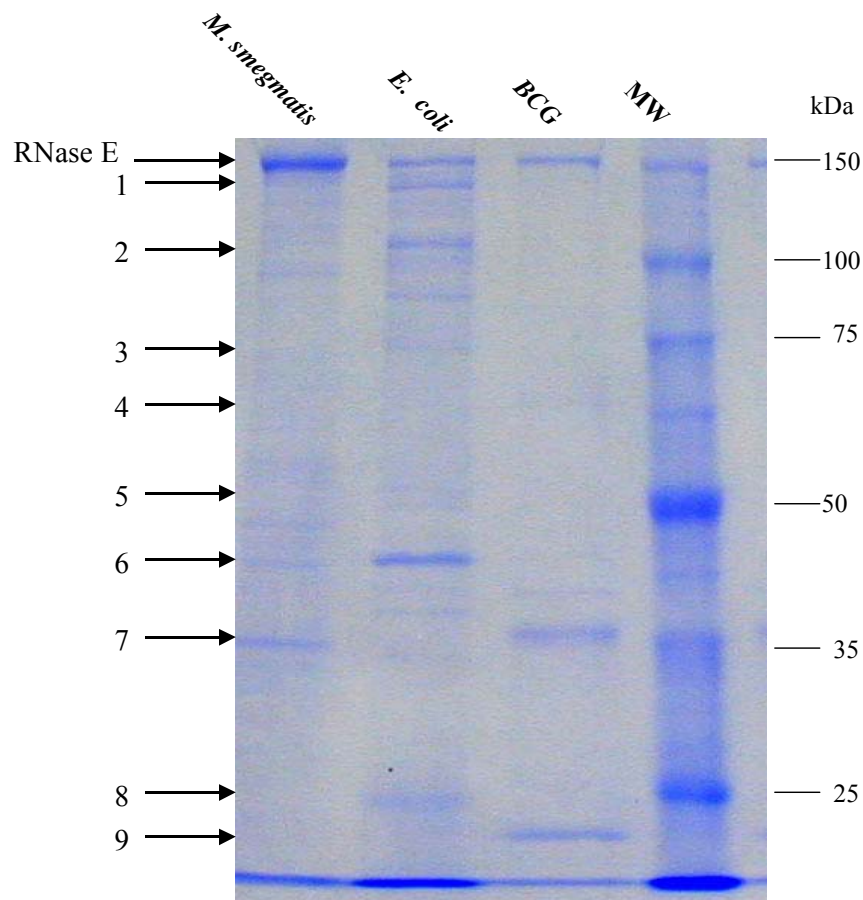
Fig. 1: SDS polyacrylamide gel (9%) electrophoresis of purified 6His-FLAG-tagged RNase E preparations from *M. smegmatis*, *E. coli* and *M. bovis* BCG. The polypeptides identified by mass spectrometry are indicated by numbers. MW: molecular weight marker.

Despite the good expression of RNase E in *M. smegmatis*, our efforts to identify the copurified proteins failed during this experiment, probably because of the lack of its complete genome sequence at that time.

Srne-associated proteins

6-His-tag labelled protein was overexpressed in *E. coli* and *M. smegmatis* and was purified from lysates of *M. smegmatis* with Talon Metal Affinity Resin. The purified preparation separated by SDS-polyacrylamide gel electrophoresis furnishes different protein bands besides RNase E (Fig. 2). These bands were cut and identified by mass spectrometry. Table I lists the identified proteins. Proteolytic fragments of RNase E were found in all bands checked. GroEL, the major associated protein, is a chaperonin, which was also found in the RNase E preparation isolated from *M. bovis* BCG. In *M. smegmatis*,

no heat shock treatment was applied during the expression of RNase E. The complex is very stable; no proteins were detected in the flow-through material when 50 000 MWCO Vivaspin concentrators were used (data not shown). GTP pyrophosphokinase takes part in signal transduction mechanisms. The negative regulator of genetic competence participates in the protein turnover and chaperone function. Dimethyladenosine transferase is an S-adenosylmethionine-dependent methyltransferase. Mutations in a gene encoding a 16S rRNA methyltransferase result in low-level streptomycin resistance in *Streptomyces coelicolor* [126]. The universal stress protein is a small cytoplasmic protein whose expression is enhanced under stress conditions and increases cell survival.

No visible differences were seen in the associated proteins when *M. smegmatis* was grown in LB or Middlebrook media.
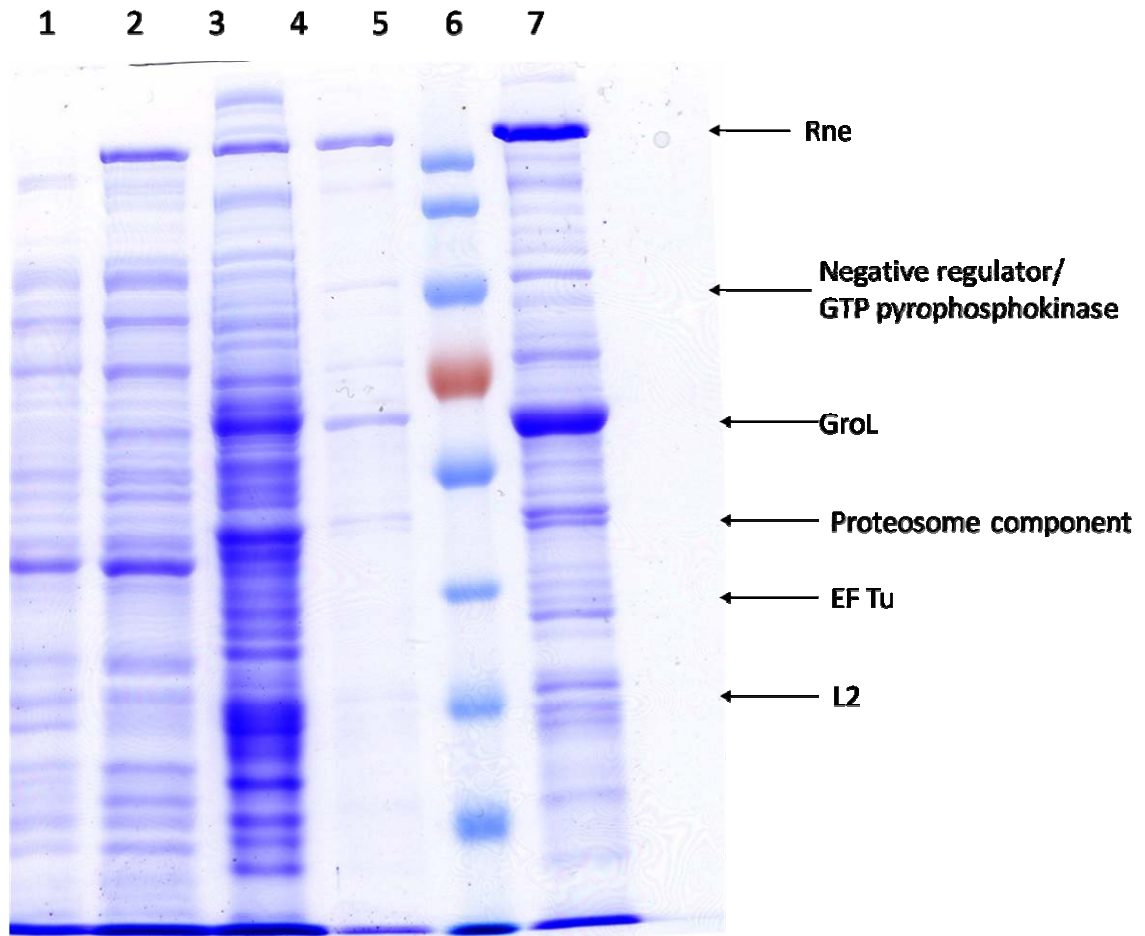
Fig. 2: Srne was overexpressed in *E. coli* and *M. smegmatis* and purified from *M. smegmatis.* The preparations of smegmatis RNase E were analysed on SDS polyacrylamide gel. The figure depicts the results of the overexpression experiments and shows the purification results, too. The first two lanes are *E. coli* extracts without and with induction. The RNase E protein has aberrant mobility as its homologues from other species. It migrates as a 180 kDa protein. Next lane is a *M. smegmatis* extract, the Srne band appears in this sample in the same position, too. After purification (lane 4), the sample contains Srne and many associated proteins. Lane 6 contains a concentrated preparation made with a 50 kDa concentrator. Last lane shows that there are no proteins in the flow-through material; even the smaller proteins remained associated to Srne.

E. coli	*M. tuberculosis*	*M. smegmatis*
• Polynucleotide phosphorylase • Enolase • Rh1B helicase	• GroEL • Inorganic polyphosphate/ATP-NAD kinase (Mb1721) • N-acetyltransferase (Mb0825c)	• Chaperonin GroL • Ribosomal proteins • Negative regulator of genetic competence • GTP pyrophosphokinase • Proteosome component • EF Tu

Table I.: Comparison of the RNase E associated proteins from different bacteria

Expression and purification of mycobacterial CafA

The sequence of *M. tuberculosis* CDC1551 contains a gene (MT2520) which codes for a protein similar to cytoplasmic axial filament proteins of other species (CafA). *E. coli* CafA was renamed ribonuclease G because of its endoribonuclease activity and certain similarity to the N-terminal portion of RNase E [72;103]. In *M. tuberculosis* CDC1551, this protein contains 661 amino acids and exhibits 100% identity with the C-terminal part of H37Rv RNase E. Classification of the RNase E/G-like proteins in terms of the relative positions of their possible catalytic versus possible scaffold regions allows an evolutionary tree to be drawn [104]. This highly correlates with the phylogenic classification made on the basis of small-subunit ribosomal RNA genes. Similar to RNase E, mycobacterial CafA, a polypeptide with the predicted molecular weight of 67 kDa, has an aberrant mobility (100 kDa) in SDS polyacrylamide gels. Likewise, its overexpression in *M. bovis* BCG and purification result (Fig. 3) in a preparation that contains a copurified inorganic polyphosphate/ATP-NAD kinase (Ppnk), a truncated form of CafA (ΔCafA) and an extra polypeptide whose identity was not determined.
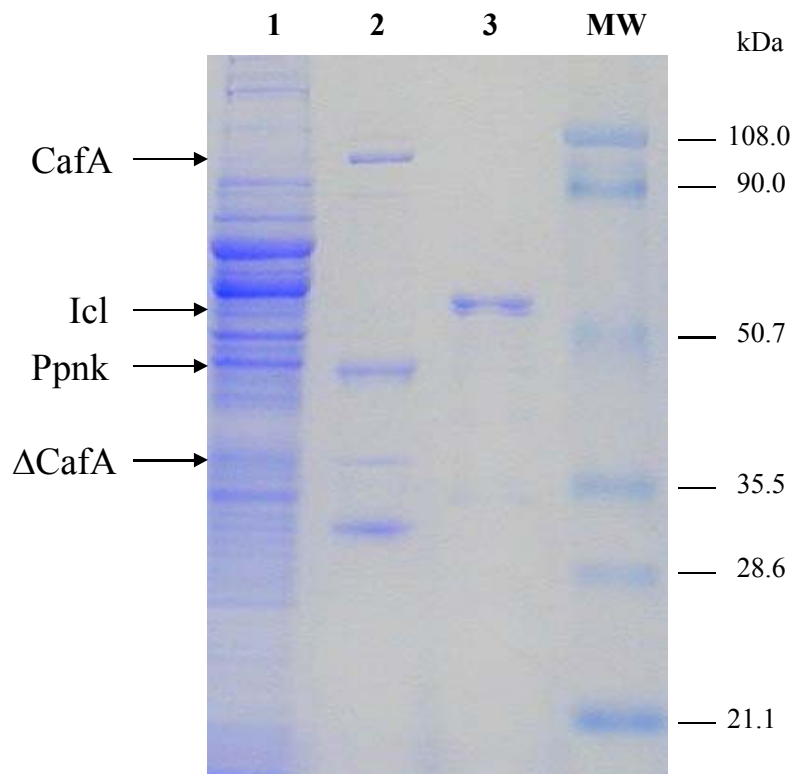
Fig. 3: Purification of CafA. The total *M. bovis* BCG extract (1), the purified CafA preparation (2) and Icl preparation (3) were analysed in a 10 % SDS polyacrylamide gel followed by Coomassie blue staining. MW: molecular weight marker. The polypeptides corresponding to the full length CafA, isocitrate lyase (Icl), an inorganic polyphosphate/ATP-NAD kinase (Ppnk), and a proteolytic form of CafA (ΔCafA) are indicated by arrows.

Expression and purification of mycobacterial RNase E/G for biochemical characterisation

To learn more about organization and biochemical properties of RNase E/G from the *M. tuberculosis*; RNase E/G homologue was overproduced in *E. coli* and purified by affinity chromatography. Since the full-length *M. tuberculosis* RNase E/G is difficult to purify in large amounts because of its tendency to form insoluble aggregates upon overexpression, we cloned its truncated form of 621 amino acids, referred to as MycRne. The amino acid sequence of MycRne includes the entire catalytic domain and the adjacent C-terminal region of this protein (Fig. 4 /A). The corresponding genomic fragment was amplified by PCR, ligated into an expression vector and verified by sequencing. The recombinant MycRne carrying a 6His-tag was overexpressed in *E. coli* strain

BL21-CodonPlus(DE3)-RIL and purified under native conditions. As seen in Fig. 4 /B, the 71 kDa MycRne protein exhibited an aberrant mobility, migrating as a 110 kDa polypeptide. Mass spectrometry analysis did not reveal any contamination of the MycRne preparation by *E. coli* RNase E/G polypeptides or other host ribonucleases (results not shown).
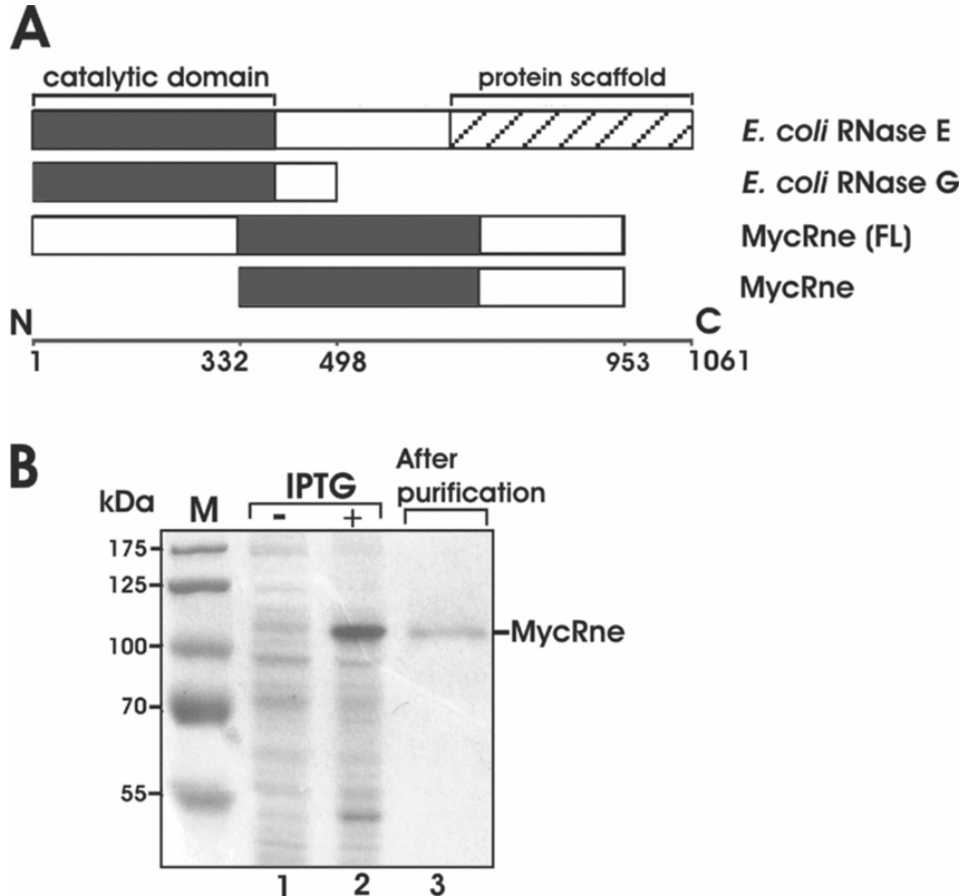

Fig. 4: (**A**) Primary structures of *E. coli* and *M. tuberculosis* RNase E/G homologues. The evolutionarily conserved minimal catalytic domain is shown by black boxes in the full-length *E. coli* RNase E, RNase G and *M. tuberculosis* RNase E/G (MycRne) polypeptides as well as in the N-terminally truncated form of *M. tuberculosis* RNase E/G used in the study. The 'protein scaffold' region (hatched box) of *E. coli* RNase E (residues 688–1061) is the location of the binding sites for the major components of the degradosome. (**B**) Purification of MycRne. Affinity-purified mycobacterial MycRne, as well as protein extracts from BL21(DE3) cells harbouring the MycRne-coding plasmid before (−) and after (+) addition of IPTG respectively, were analysed in SDS/10% polyacrylamide gels followed by Coomassie Blue staining. Indicated are the positions of *M. tuberculosis* RNase E/G (MycRne) and the molecular-mass markers (in kDa; lane M).

Quaternary structure of *M. tuberculosis* RNase E/G

The putative catalytic domain of MycRne contains the highly conserved Zn-link motif known to be implicated in dimerization and tetramerization of *E. coli* RNase E/G

[89;90]. To assess whether the ability of RNase E/G homologues to form dimeric and tetrameric forms is evolutionarily conserved, we analysed the oligomerization state of affinity-purified MycRne. According to the calibration profile obtained with aldolase, BSA and chymotrypsinogen A, MycRne was eluted as a complex with a hydrodynamic radius corresponding to a spherical protein with an apparent molecular mass of approx. 325 kDa (Fig. 5 /A), suggesting that, similar to *E. coli* homologues, MycRne may exist in a tetrameric form. In order to confirm the oligomerization state of MycRne by an independent method, analytical ultracentrifugation was performed (Fig. 5 /B).
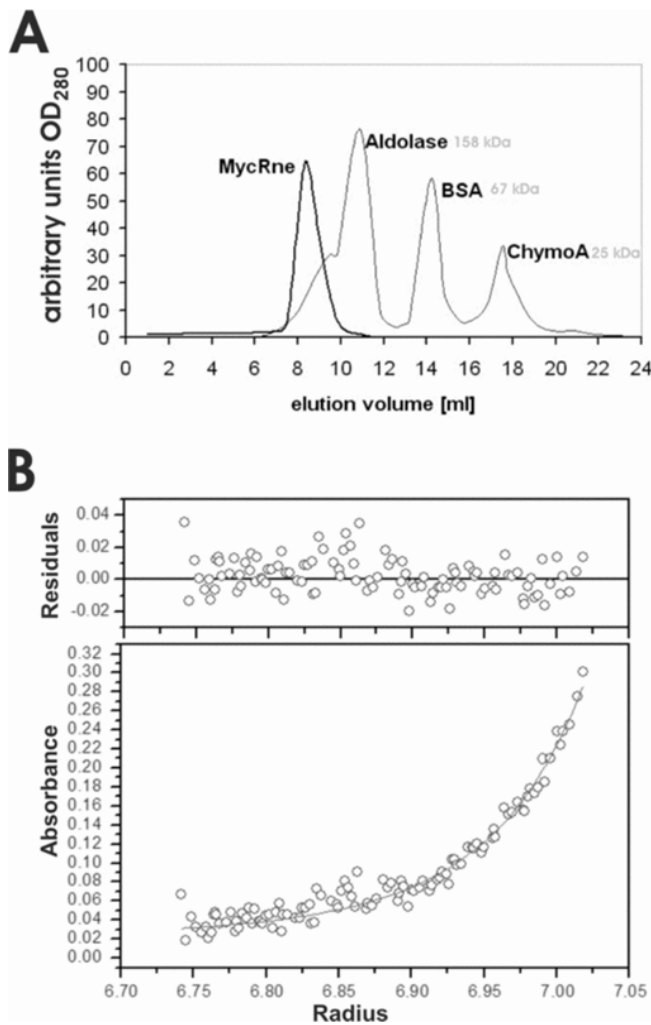
Fig. 5: Quaternary structure of RNase E/G

(**A**) Gel filtration of MycRne. Affinity-purified MycRne (thicker line) was analysed by size-exclusion chromatography. The column was calibrated with aldolase (158 kDa), BSA (67 kDa) and chymotrypsinogen A (25 kDa) (thinner line). The absorbance at 280 nm is indicated on the *y*-axis, whereas elution volumes are indicated on the *x*-axis. (**B**) Sedimentation equilibrium analysis. A representative radial concentration distribution of RNase E/G at 16 µM is shown after reaching equilibrium (18 h) at 12000 rev./min at 20 °C. The lower panel plots the absorbance at 292 nm against the radial position (cm). The absorbance offset was set to 0.022 absorbance unit. The best fit of the data set (six speeds, 1502 points) was consistent at this sample concentration with monomer–dimer equilibrium (solid lines) with a K_d of 1.8 µM. Residual values between experimental data and a self-associating model of ideal species (molecular mass, 71100 Da) are shown in the upper panel.

Cleavage of oligonucleotide substrates

To test whether MycRne has an endoribonucleolytic activity and to compare its specificity with that of *E. coli* RNase E, we performed cleavage assays using affinity-purified MycRne and Rne498 (*E. coli* RNase E; residues 1–498), a C-terminally truncated

form of *E. coli* RNase E representing its catalytic domain [93]. The assays were carried out with synthetic ribo-oligonucleotides BR10, 9SA and OmpC, all of which are well-characterized *E. coli* RNase E substrates [120;127;128]. As seen in Fig. 6, MycRne could cut all three oligonucleotides yielding cleavage patterns that were largely indistinguishable from the analogous patterns generated by its *E. coli* counterpart. A minor difference was only observed in the cleavage pattern of OmpC. Although Rne498 cleaved this oligonucleotide at positions 5 and 6 with equal efficiencies, MycRne showed some preference for cleavage at position 5. We also found that, similar to its RNase E/G homologues from *Aquifex aeolicus* and *E. coli*, MycRne requires Mg^{2+} ions for its activity (Fig. 6 /E).
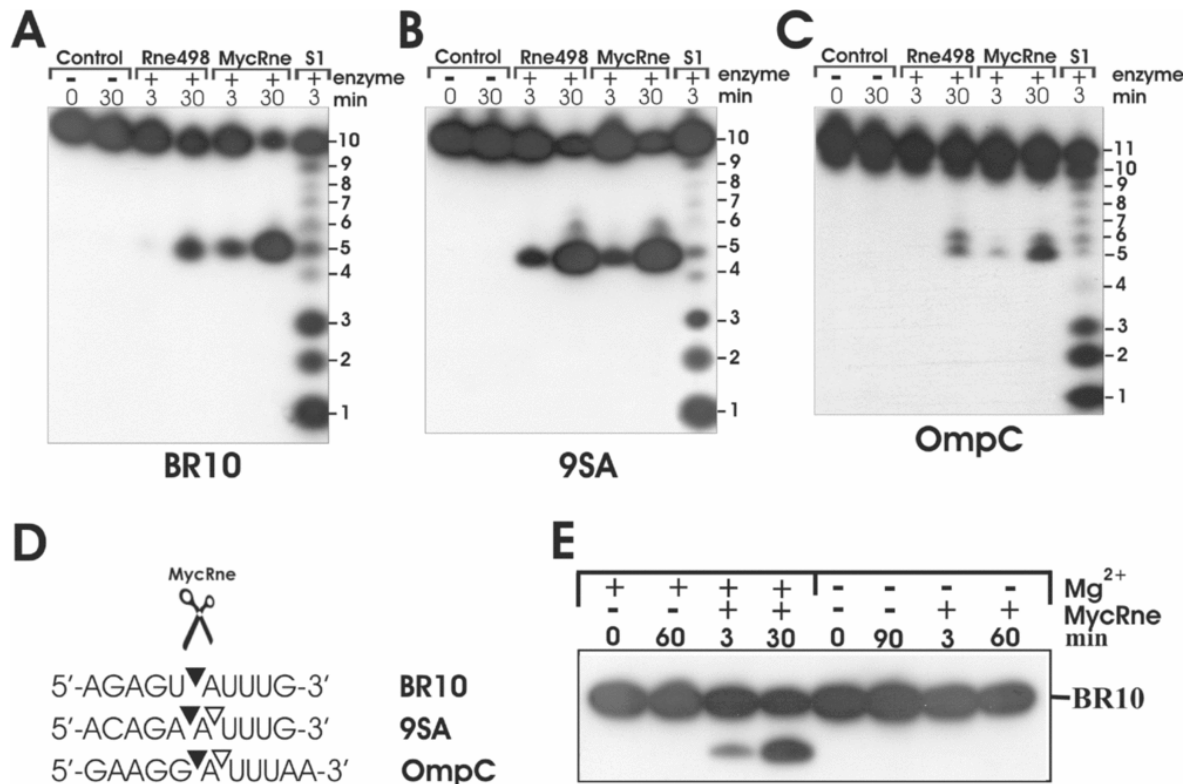
Fig. 6: Cleavage patterns of oligonucleotides BR10, 9SA and OmpC

Each 5′-end-labelled oligonucleotide (**A**, **B** and **C** respectively) was incubated without enzyme (control), affinity-purified *E. coli* RNase E (Rne498) or *M. tuberculosis* RNase E/G (MycRne), and aliquots withdrawn at the times indicated above each lane were analysed on 20% polyacrylamide/urea gels. Lanes S1, 1 nt ladder generated by partial digestion of BR10, 9SA or OmpC with S1 nuclease respectively. The sequence of BR10, 9SA and OmpC is shown in (**D**). The internucleotide bonds that are sensitive to MycRne cleavage are indicated by triangles. Filled triangles point towards the bonds that have higher sensitivity to the endonucleolytic activity of MycRne. (**E**) Magnesium-dependence of MycRne cleavages. BR10 was incubated with MycRne in the absence (−) or presence (+) of Mg^{2+} ions, and aliquots withdrawn at times indicated above each lane were analysed on a 15% sequencing gel.

5′-end-dependence of *M. tuberculosis* RNase E/G cleavages

RNase E/G homologues from Gram-negative bacteria are known to preferentially cleave 5′-monophosphorylated substrates over non-phosphorylated [102;129;130] or 5′-triphosphorylated ones [131]. Employing 5′-monophosphorylated and non-phosphorylated BR13 (5′-GGGACAGUAUUUG-3′) tagged with a fluorescein group at their 3′ ends, we demonstrated that, similar to its counterparts, MycRne cleaves 5′-monophosphorylated substrates faster than the non-phosphorylated ones (Fig. 7 /A and B). Thus our findings suggest that the so-called 5′-end-dependence is apparently a

common feature of RNase E/G homologues from both Gram-negative and Gram-positive bacteria.
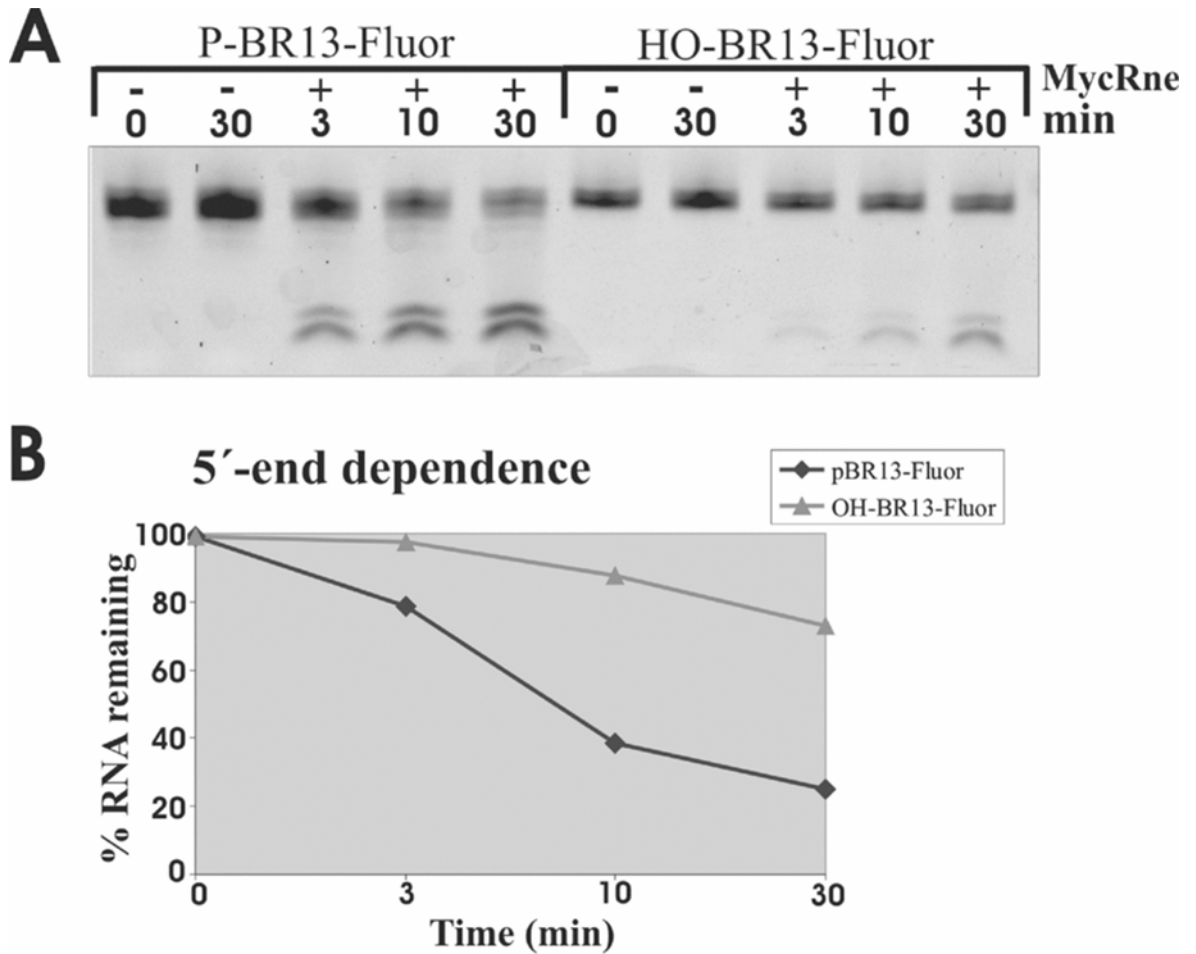

Fig. 7: 5′-end-dependence of MycRne cleavages

(**A**) Relative efficiency of MycRne cleavage of fluorescently labelled 5′-phosphorylated and non-phosphorylated oligonucleotides (P-BR13-Fluor and HO-BR13-Fluor respectively). Each oligonucleotide (~5 pmol) was incubated without (control) or with affinity-purified MycRne, and aliquots withdrawn at the times indicated above each lane were analysed on a 15% (w/v) sequencing gel. (**B**) Graphical representation of uncleaved RNA (%) plotted as a function of time (min) indicates that MycRne cleaves the 5′-phosphorylated substrate faster than the non-phosphorylated one.

Probing the substrate specificity of *M. tuberculosis* RNase E/G

In order to identify specific sequence determinants of MycRne cleavage sites, we used essentially the same oligonucleotide-based approach that was employed previously to characterize its *E. coli* counterpart [132]. By comparing the cleavage patterns of poly(A) and poly(U) oligonucleotides and their mutant variants carrying single-base substitutions of G, C, U or A respectively for adenosine (or uridine), this method allows

determination of each nucleotide's effect at multiple positions to the point of cleavage [132].

Unlike *E. coli* RNase E [133;134], MycRne cleaved A27 inefficiently. As seen in (Fig. 8 /A), despite a 5-fold excess of MycRne (when compared with the cleavage conditions of U27), A27 cleavage products can be readily detected only on overexposed X-ray films (Fig. 8 /A). In the following assays, we therefore decided to use only U27 (control) and its derivatives, U27A, U27G, U27C and U27ab oligonucleotides, that had a single-base substitution of A, G, C or abasic residue respectively for U at position 14.
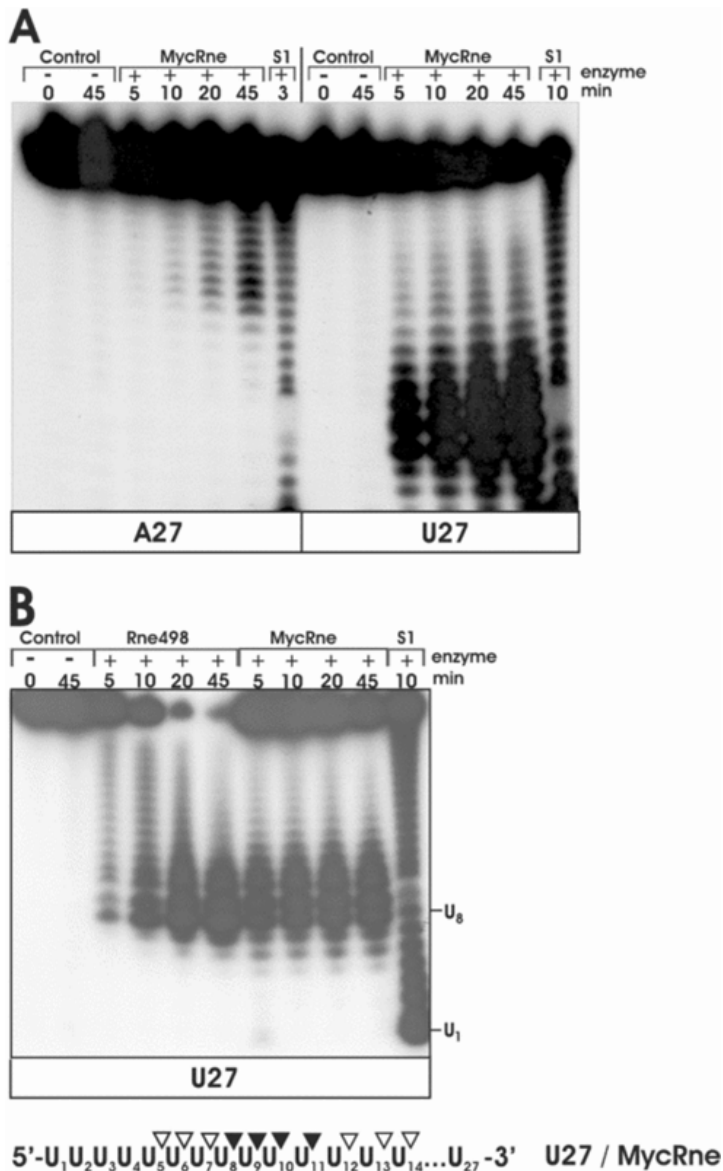
Fig. 8: Comparative cleavage of A27 and U27 by MycRne

(**A**) 5′-End-labelled A27 (left) or U27 (right) were incubated without enzyme (control) or with MycRne, and aliquots withdrawn at the times indicated above each lane were analysed on 15% polyacrylamide/urea gels. (**B**) Cleavage patterns of U27 generated by Rne498 and MycRne. 5′-End-labelled U27 was incubated without enzyme (control), with *E. coli* RNase E (Rne498) or with MycRne, and aliquots withdrawn at the times indicated above each lane were analysed on a 15% polyacrylamide/urea gel. The co-ordinates of U_1 and U_8 within U27 are indicated. Internucleotide bonds with a moderate (open triangles) or high (closed triangles) sensitivity to MycRne cleavage are indicated in a schematic view of U27 shown at the bottom.

Similar to cleavage of U27 (Fig. 8 /B), incubation of U27G with MycRne and Rne498 resulted in nearly identical patterns (Fig. 9 /A). The major cleavages of U27G at positions U8, U9, U10 and U15 were observed for both enzymes, whereas Rne498 (but

not MycRne) could additionally cleave this substrate at position U18. In the case of
E. coli RNase E, it has been reported previously that a G nucleotide, which is 5′ and in
close vicinity to the scissile bond, is an important determinant of cleavage [128;130;132].
Likewise, we found that *M. tuberculosis* RNase E/G cleavage is more efficient if there is
a G nucleotide located two nucleotides upstream of the scissile bond (Fig. 9 /A). These
data are fully consistent with the cleavage patterns of BR10, 9SA and OmpC
oligonucleotides, showing that MycRne cleavage frequently occurs two nucleotides
downstream of a G nucleotide (Fig. 6).

In contrast with nearly identical cleavage patterns that were generated by MycRne
and Rne498 using U27G (Fig. 9 /A), the cleavage patterns of U27A, U27C and U27ab
showed relatively low resemblance (Fig. 9 /B, C and D respectively). Although Rne498
can cut at multiple positions within U27A (Fig. 9 /B), MycRne cleavage of the same
substrate was not observed at many of these locations, especially downstream and
upstream of U16. Similarly, the presence of a cytosine at position 14 in U27C (Fig. 9 /C)
strongly inhibits MycRne (and to a lesser degree Rne498) cleavage at nearly all locations,
suggesting the overall inhibiting effect of this nucleotide. Finally, we found that
substitution of an abasic residue for the U at position 14 in U27ab (Fig. 9 /D) decreased
the efficiency of MycRne cleavage at multiple locations. This finding strongly suggests
that the presence of uridines at many locations close to the scissile bond promotes
MycRne cleavage.

On the basis of the above experimental data, we determined and summarized the
effects of each nucleotide within MycRne cleavage sites (Fig. 9 /E). Interestingly,
according to these data, the C at position +2 in 9SA should confer higher resistance of this
oligonucleotide (in comparison with BR10 lacking a cytosine at the equivalent position)
to MycRne. In contrast, we did not observe any significant differences in the efficiency of
cleavage (Fig. 6, and M.-E. Zeller and V. R. Kaberdin, unpublished work). This may
imply that the expected inhibiting effect of the cytosine was efficiently counteracted by
other nucleotides, for example by the A and G nucleotides at positions −3 and −2
respectively. In other words, strong enhancing effects of nucleotides at certain positions
of different cleavage sites can potentially neutralize or override negative effects of other
sequence determinants, resulting in approximately equal efficiency of cleavage.

As in the case of *E. coli* RNase E [132;134], the efficiency of MycRne cleavage of
U27 and its mutant variants decreases with the number of the remaining nucleotides that

are 5′ to the scissile bond (the 'end-proximity effect'), thereby leading to accumulation of short oligomers that are further resistant to the nucleolytic activity of this enzyme.
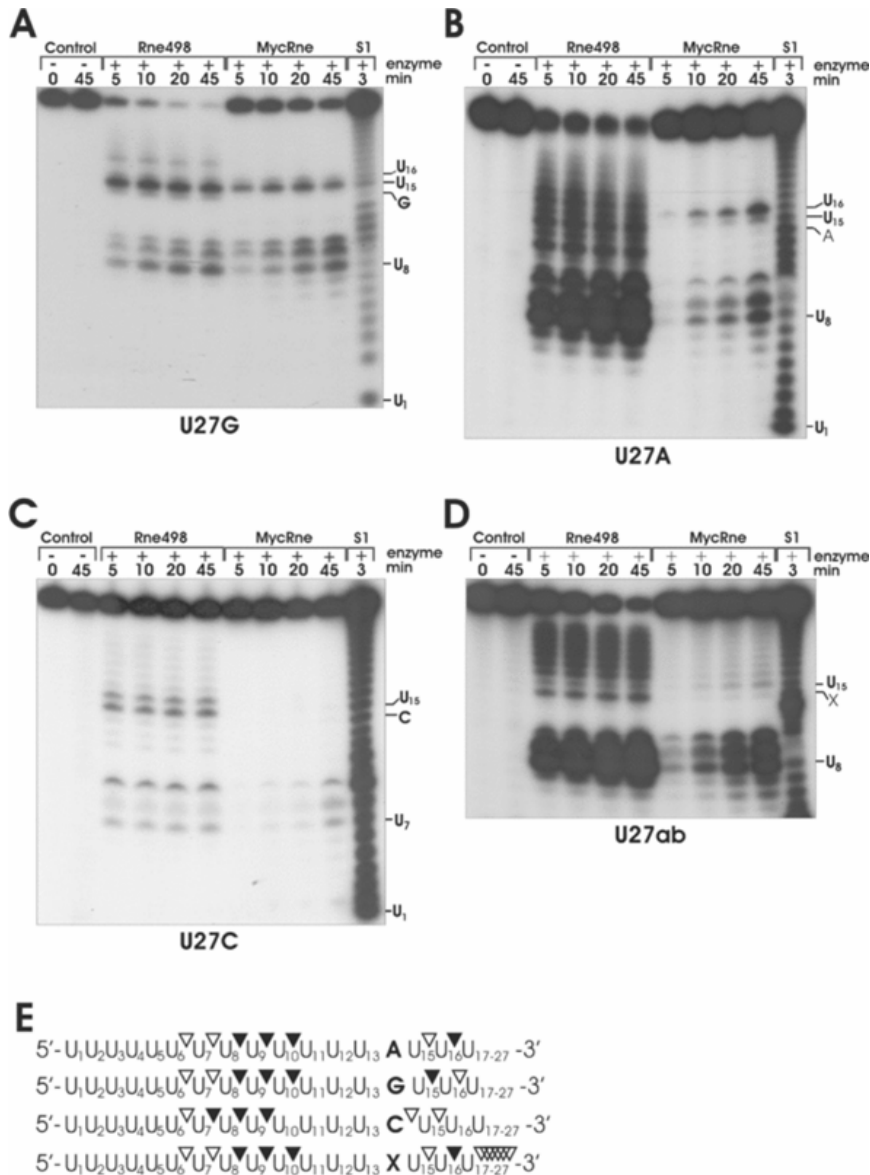
Fig. 9: Cleavage patterns of U27G, U27A, U27C and U27ab generated by Rne498 and MycRne

Each 5′-end-labelled substrate derived from U27 by replacement of the U at position 14 by a G (U27G) (**A**), A (U27A) (**B**), C (U27C) (**C**) or abasic (U27ab) (**D**) residue was incubated without enzyme (control), with *E. coli* RNase E (Rne498) or with *M. tuberculosis* RNase E/G (MycRne), and aliquots withdrawn at the times indicated above each lane were analysed on 15% polyacrylamide/urea gels. Indicated are the positions of several nucleotides including the substituted base [A, G, C or the abasic residue (X) respectively] as well as site(s) sensitive to MycRne cleavage. (**E**) Schematic views of the substrates. The internucleotide bonds with a moderate and high susceptibility to MycRne cleavage are depicted by open and closed triangles respectively.

9S RNA processing by *M. tuberculosis* RNase E/G

RNase E is playing an essential role in maturation of stable RNAs in *E. coli*; it is known to process the 9S RNA precursor of the 5S rRNA [73]. To find out whether MycRne might act likewise in the processing of rRNA in *M. tuberculosis*, we examined the cleavage pattern obtained after incubation of *in vitro* transcribed *M. tuberculosis* 9S RNA with Rne498 and MycRne. Although both enzymes could cleave this RNA, the cleavages occurred at different locations (Fig. 10 /A). This finding is consistent with our data (Fig. 9) suggesting some differences in the substrate specificities of *E. coli* and *M. tuberculosis* RNase E/G homologues. Further analysis (Fig. 10 /B) revealed that MycRne cleaved 9S RNA at the position, which nearly coincides with the position of the 5′-end of mature 5S rRNA *in vivo*, which was mapped by primer extension of total RNA (Fig. 10 /B and C).
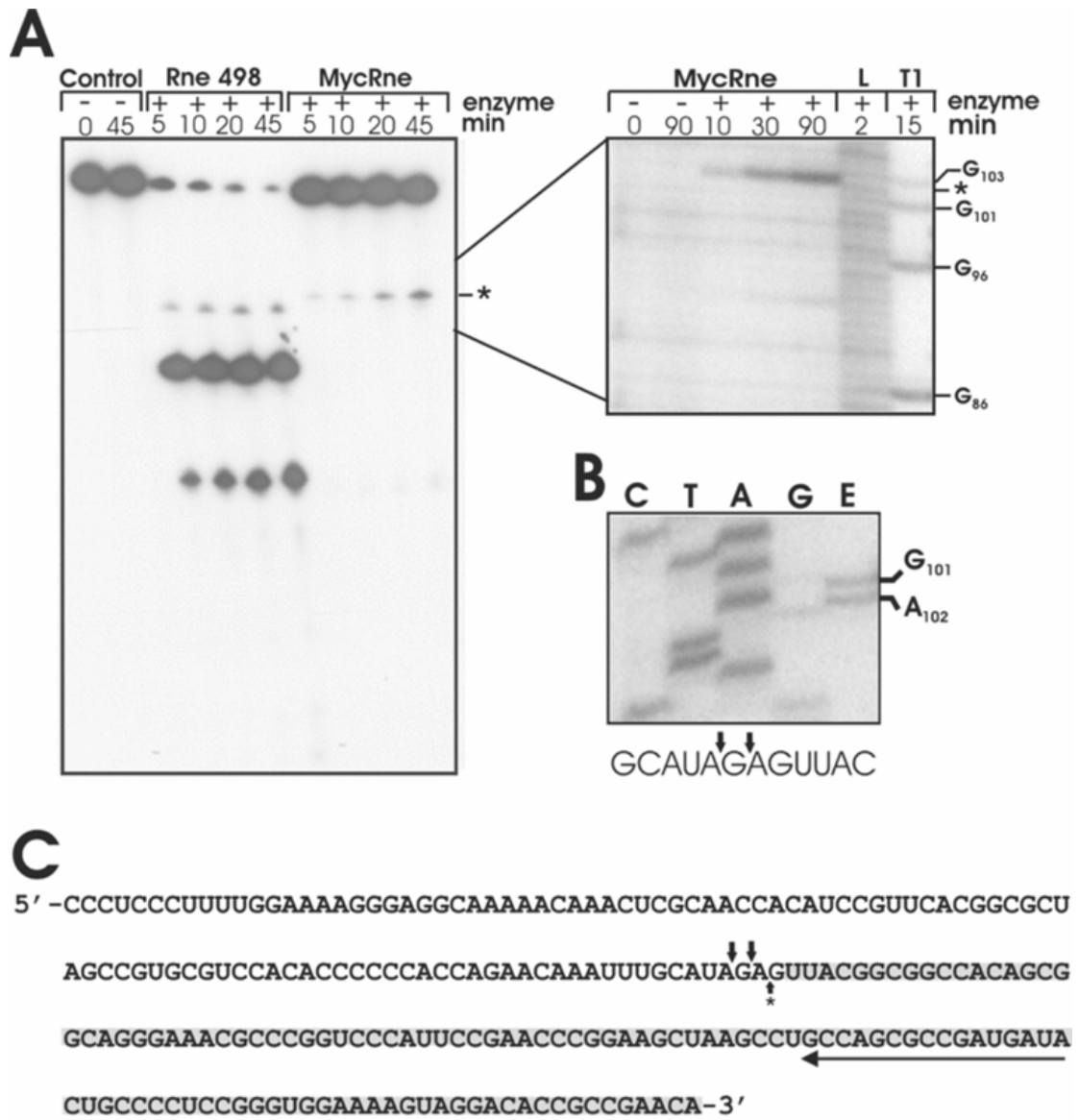
Fig. 10: 9S RNA processing *in vitro* and *in vivo*

(**A**) 5'-end-labelled mycobacterial 9S RNA was incubated without enzyme (control), with *E. coli* RNase E (Rne498) or with *M. tuberculosis* RNase E/G (MycRne). The position of the *M. tuberculosis* RNase E/G cleavage site (*) was determined employing concomitantly run partial alkaline (L) and RNase T1 (T1) digests of the same transcript shown on the right. (**B**) Primer-extension analysis of total mycobacterial RNA (lane E) was performed using a 5'-^{32}P-labelled primer specific for 5S rRNA. The 5'-end of the in vivo processed 5S rRNA was determined by employing a concomitantly run sequencing ladder (lanes C, T, A and G) generated with the same primer. (**C**) The sequence of *M. tuberculosis* 5S rRNA (highlighted with grey shading) and its 5'-end-flanking region. A long horizontal arrow shows the direction and position of the primer used for primer extension. The position of in vitro (**A**) and in vivo (**B**) MycRne cleavage sites that were mapped close to the 5'-end of 5S rRNA are indicated by a single upward and two downward arrows respectively.

Discussion

It has been more than 30 years since the introduction of a novel compound for the treatment of tuberculosis. New drugs are extremely needed. Agents that reduce the duration and complexity of the current therapy would have a major impact on compliance and overall cure rate. In recent years, our understanding of the tubercle bacillus and its interaction with the human host has improved dramatically, particularly with the publication in 1998 of the complete genome sequence of *M. tuberculosis* H37Rv [111]. New genetic tools have been developed and we can now ascertain the function of individual genes. Thus, many potential drug targets can be identified.

Mycobacteria are very successful pathogens, which are able to survive under adverse conditions like long non-replicating persistence, intracellular survival. Dynamic regulation of RNA decay and processing should be a very important factor in adapting to environmental changes. Over the past years it became obvious that mRNA degradation is a very important step in regulation of prokaryotic gene expression.

Given the central role of RNase E in RNA processing and decay in *E. coli*, it is conceivable that the RNase E-dependent regulation of RNA stability in mycobacteria might also be a very important mechanism, adjusting the cellular metabolism to environmental changes. Adaptive processes in the RNA metabolism of latent mycobacteria differentially affect the steady-state levels of numerous transcripts [135], ribosome biosynthesis [136] as well as RNase E/G levels [137], suggesting an important regulatory role of this enzyme during disease development.

We focus our work on mycobacterial RNase E like proteins; the results are the first steps towards understanding their structure, function and the role of bacterial metabolism.

Although *M. tuberculosis* and related species are considered to be members of Gram positive bacteria, the mechanisms of RNA decay and processing in these organisms are apparently different from the regulatory circuits that control RNA metabolism in Gram positive bacteria with a low GC content such as *Bacillus subtilis*. The latter lacks RNase E and RNase G (CafA) and therefore the mechanisms that regulate RNA stability in *B. subtilis* must be quite different from those taking place in mycobacteria [105;138]. On the other hand, RNase E can be found in the majority of human pathogens (both Gram positive and Gram negative bacteria), where it seems to be a key enzyme in RNA processing and degradation.

In our work we cloned, expressed and purified the RNase E/G homologue from *M. tuberculosis* (MycRne) and *M. smegmatis* (Srne) and identified associated proteins. RNase E and RNA helicase B play central roles in the cytoskeletal organization of the degradosome in *E. coli* [98]. Polynucleotide phosphorylase and enolase are also important components. In agreement with a previously proposed idea [91], the associated proteins can be different in other bacteria.

In the RNase E preparation isolated from *M. bovis* BCG (Fig. 1), chaperonin GroEL (band 4) was identified. Bands 7 and 9 are the products of genes Mb1721 and Mb0825c, respectively. These proteins were found in the database as hypothetical proteins. Mb1721 is equivalent to Rv1695 (100 % identity) from *M. tuberculosis* H37Rv. This protein is an inorganic polyphosphate/ATP-NAD kinase (Ppnk) and it is playing a crucial role in the regulation of NAD/NADP level and in biosynthetic reactions in the cell. Its association with RNase E may play a regulatory role by helping to adapt to environmental changes. Mb0825c is equivalent to Rv0802c of *M. tuberculosis* H37Rv. The protein displays partial similarity with many acetyltransferases and hypothetical proteins.

When 6-His-tag labelled proteins from lysates of *M. smegmatis* were purified (Fig. 2) also GroEL was the major associated protein. However ribosomal proteins were also present. Among others, a negative regulator of genetic competence and a GTP pyrophosphokinase, which has role in cellular response to starvation, dimethyladenosine transferase and the universal stress protein were also component of the complex.

The copurified proteins from *M. smegmatis* were different from those in *E. coli*, as expected after previous mycobacterial studies, though surprisingly they were not even identical to the associated proteins we found in case of the RNase E/G homologue from *M. tuberculosis*. Interestingly much more proteins were detected in the *M. smegmatis* preparates, than in the ones from *M. tuberculosis*. Although it is not easy to determine whether the associated proteins we report from *M. smegmatis* are specific functional components or occasional contaminants, it is important to note that the overexpression and subsequent purification of isocitrate lyase [112] has yielded nearly pure recombinant protein, indicating that the above described copurification is specific and is not dependent on the presence of the 6HisFLAG tag.

While there is strong homology in the catalytic part of RNase E enzymes among mycobacteria, the C-terminal portions are quite different. In silico, using the CLC Combined Workbench the secondary structure of the RNase E from *M. smegmatis* and

M. tuberculosis was drawn. Srne is mostly helical protein, containing 30 α-helices and with Pfam analysis 22 potential domains were suggested, with 9 domains more, than what was predicted in the tuberculosis RNase E.

The in silico results suggest that there are possible differences among mycobacteria in the structure of the enzyme, which could explain the difference in quality and quantity of the associated proteins.

Despite the use of protease inhibitors in addition to the full-length RNase E its proteolytic fragments were detected in all bands. *E. coli* RNase E is also very sensitive to proteolysis [96]. The presence of PNPase and RhlB helicase could not be detected among the copurified proteins. The *M. smegmatis* genome contains genes coding for PNPase (MSMEG_2656) and RhlB helicase (MSMEG_1930). The proteins we found as associated proteins take part in protein synthesis, regulation and the stress response.

Our data indicate that, similar to *E. coli* [96], mycobacterial RNase E/G homologues are able to copurify with other proteins. However, in agreement with the previously proposed idea [91], the nature of the associated proteins is different when compared to the composition of the *E. coli* RNase E complex [95;96;97]. Further studies are needed to address the role of the identified proteins in relation to the specific steps of RNA metabolism in mycobacteria and their regulation by environmental factors.

To learn more about the function and biochemical properties of the RNase E/G homologue from *M. tuberculosis* (MycRne), we cloned, purified and characterized a polypeptide including the centrally located catalytic domain as well as the flanking C-terminal part of this protein (Fig. 4).

By employing oligonucleotide substrates, we have also shown that MycRne has an endoribonucleolytic activity, which is dependent on the 5′-phosphorylation status of its substrates, thereby suggesting that MycRne is a 5′-end-dependent endoribonuclease. This property of MycRne and other RNase E/G homologues [84;102;129;131;139] implies that these enzymes more efficiently cleave already damaged or partially degraded forms of cellular RNAs (i.e. RNA species that usually carry 5′-monophosphate groups) rather than primary transcripts, which are naturally triphosphorylated.

Given that RNase E and RNase G are involved in maturation of ribosomal and transfer RNAs in *E. coli* [83;140], we anticipated that this function of RNase E/G-like proteins might be also conserved in mycobacteria. Indeed, we found that MycRne was able to cleave mycobacterial 9S RNA (Fig. 10 /A), a putative precursor of its cognate 5S rRNA, and the cleavage occurred in close vicinity to the mature 5′-end of 5S rRNA

(Fig.10j /B and C), thereby suggesting a role for this enzyme in rRNA processing. Although the internucleotide bonds at the 5′-end of 5S rRNA that are generated by MycRne *in vitro* (Fig. 10 /A) and during rRNA processing *in vivo* (Fig. 10 /B) were not exactly the same, this minor (one or two nucleotide) difference could be well explained by the action of ancilliary factors or associated ribosomal proteins that can affect MycRne cleavage *in vivo* and therefore slightly influence the selection of the scissile bond(s).

Conclusions

Mycobacteria are very successful pathogens; they are able to survive under adverse conditions. Dynamic regulation of RNA decay and processing should be a very important factor in adapting to environmental changes. Over the past years it became obvious that mRNA degradation is a very important step in regulation of prokaryotic gene expression.

It has been more than 30 years since the introduction of a novel compound for the treatment of TB. New drugs are extremely needed. Given the central role of RNase E in RNA processing and decay in *E. coli* and other bacteria, it is conceivable that the RNase E-dependent regulation of RNA stability in mycobacteria might also be a very important mechanism, adjusting the cellular metabolism to environmental changes.

We focus our work on mycobacterial RNase E like proteins. We cloned RNase E from *M. tuberculosis*, *M. bovis* BCG and *M. smegmatis*, expressed and purified the proteins, identified associated proteins and characterised enzyme activities. Our results are the first steps towards the understanding of RNA metabolism in mycobacteria and could make finding new drug targets possible. Further studies are needed to address the specific roles of the associated proteins in relations to the specific steps of RNA metabolism in mycobacteria and their regulation by environmental factors.

Acknowledgements

I would like to express my gratitude to all those who have given me the possibility to carry out research work and prepare this thesis.

I express my deepest thanks to my supervisor, András Miczák for his invaluable scientific guidance and encouragement.

I am particularly grateful to Vladimir Kaberdin for his skilful guidance, support and for granting me the possibility to spend 7 months in his laboratory in the Max F. Perutz Laboratories, University of Vienna and to learn new and unique methods in enzimology.

I would like to thank to Professor Yvette Mándi, Head of the Department of Medical Microbiology and Immunobiology, Faculty of Medicine, University of Szeged, for accepting me as PhD student.

I also owe my thanks to Valéria Endrész and Katalin Burián for their support and for allowing me to participate in their upcoming project and giving me the opportunity to learn some of the required methods.

I thank to Mrs Lévai for her excellent technical assistance and advice.

I am grateful to Ildiko Faludi and Tania Lombo, with whom I had the opportunity to work, during which they provided me with great pieces of advice and encouraged me, whenever I needed it the most.

Last but not least I wish to thank my whole family and friends for the indispensable help, their infinite patience, understanding, support and love.

References

1. Wells WF: Airborne Contagion and Air Hygiene, Cambridge, MA, Harvard University Press, 1955.

2. Brain JD, Godleski JJ, Sorokin SP: Quantification, origin and fate of pulmonary macrophages. In: Brain JD, Proctor DF, Reid LM, ed. Respiratory Defense Mechanisms: Part II, New York: Marcel Dekker; 1977:849-892.

3. Stead WW, Bates JH: Evidence of a silent bacillemia in primary tuberculosis. Ann Intern Med 1971; 74:559-561.

4. Flynn JL, Chan J: Immunology of tuberculosis. Annu Rev Immunol 2001; 19:93-129.

5. Schell RF, Ealey WF, Harding GE, et al: The influence of vaccination on the course of experimental airborne tuberculosis in mice. J Reticuloendothel Soc 1974; 16:131-138.

6. [Anonymous]. 2004. World health report 2004: changing history. WHO. Geneva, Switzerland. http://www.who.int/whr/2004/en/report04_en.pdf.

7. Corbett, E.L., et al. The growing burden of tuberculosis: global trends and interactions with the HIV epidemic. Arch. Intern. Med. 2003;163:1009–1021. doi: 10.1001/archinte.163.9.1009.

8. [Anonymous]. 2007. Global tuberculosis control — surveillance, planning, financing. WHO. Geneva, Switzerland. http://www.who.int/tb/publications/global_report/2007/download_centre/en/index.html

9. Koch, R. Fortsetzung der mittheilungen uber ein heilmittel gegen tuberculose. Dtsch. Med. Wochenschr. 1891;17:101–102.

10. Ehrlich, P. Aus dem Verein fur innere Medicin zu Berlin — Sitzung vom 1 Mai. Dtsch. Med. Wochenschr. 1882;8:269–270.

11. Matteelli, A., et al. Multidrug-resistant and extensively drug-resistant *M. tuberculosis*: epidemiology and control. Expert Rev. Anti Infect. Ther. 2007;5:857–871. doi: 10.1586/14787210.5.5.857.

12. Madebo, T.; Lindtjorn, B. Delay in treatment of pulmonary tuberculosis: an analysis of symptom duration among Ethiopian patients. Med. Gen. Med. 1999:E6.

13. Liam, C.K.; Tang, B.G. Delay in the diagnosis and treatment of pulmonary tuberculosis in patients attending a university teaching hospital. Int. J. Tuberc. Lung Dis. 1997;1:326–332.

14. Ewer K, Deeks J, Alvarez L, et al. Comparison of T-cell-based assay with tuberculin skin test for diagnosis of *M. tuberculosis* infection in a school tuberculosis outbreak. *Lancet* 2003; **361:** 1168–73.

15. Liebeschuetz S, Bamber S, Ewer K, Deeks J, Pathan AA, Lalvani A. Diagnosis of tuberculosis in South African children with a T-cell-based assay: a prospective cohort study. *Lancet* 2004; **364:** 2196–203.

16. Moll, A., et al. 2006. Identification of a multi-drug resistant tuberculosis cluster as a cause of death among HIV co-infected patients in rural South Africa [abstract 795]. Paper presented at the 13th Conference on Retroviruses and Opportunistic Infections. February 5–8. Denver, Colorado, USA.

17. [Anonymous]. From the Centers for Disease Control. Nosocomial transmission of multidrug-resistant tuberculosis among HIV-infected persons — Florida and New York, 1988–1991. JAMA. 1991;266:1483–1485. doi: 10.1001/jama.266.11.1483.

18. Cunningham, J., and Perkins, M. 2006. Diagnostics for tuberculosis: global demand and market potential. WHO. Geneva, Switzerland. http://whqlibdoc.who.int/publications/2006/9241563303_eng.pdf.

19. Caviedes L, Lee TS, Gilman RH, et al. Rapid, effi cient detection and drug susceptibility testing of *M. tuberculosis* in sputum by microscopic observation of broth cultures. The Tuberculosis Working Group in Peru. *J Clin Microbiol* 2000; **38:** 1203–08.

20. Moore DA, Evans CA, Gilman RH, et al. Microscopic-observation drug-susceptibility assay for the diagnosis of TB. *N Engl J Med* 2006; **355:** 1539–50.

21. Morgan M, Kalantri S, Flores L, Pai M. A commercial line probe assay for the rapid detection of rifampicin resistance in *M. tuberculosis*: a systematic review and meta-analysis. *BMC Infect Dis* 2005; **5:** 62.

22. Jindani A, Nunn AJ, Enarson DA. Two 8-month regimens of chemotherapy for treatment of newly diagnosed pulmonary tuberculosis: international multicentre randomised trial. *Lancet* 2004; **364:** 1244–51.

23. el-Sadr WM, Perlman DC, Matts JP, et al. Evaluation of an intensive intermittent-induction regimen and duration of short-course treatment for human immunodefi ciency virus-related pulmonary tuberculosis. Terry Beirn Community Programs for

Clinical Research on AIDS (CPCRA) and the AIDS Clinical Trials Group (ACTG). *Clin Infect Dis* 1998; **26:** 1148–58.

24. Zignol M, Hosseini MS, Wright A, et al. Global incidence of multidrug-resistant tuberculosis. *J Infect Dis* 2006; **194:** 479–85.

25. Vernon A, Burman W, Benator D, Khan A, Bozeman L. Acquired rifamycin monoresistance in patients with HIV-related tuberculosis treated with once-weekly rifapentine and isoniazid. Tuberculosis Trials Consortium. *Lancet* 1999; **353:** 1843–47.

26. Ginsburg AS, Sun R, Calamita H, Scott CP, Bishai WR, Grosset JH. Emergence of fluoroquinolone resistance in *M. tuberculosis* during continuously dosed moxifl oxacin monotherapy in a mouse model. *Antimicrob Agents Chemother* 2005; **49:** 3977–79.

27. Kam KM, Yip CW, Cheung TL, Tang HS, Leung OC, Chan MY. Stepwise decrease in moxifl oxacin susceptibility amongst clinical isolates of multidrug-resistant *M. tuberculosis*: correlation with ofl oxacin susceptibility. *Microb Drug Resist* 2006; **12:** 7–11.

28. Hugonnet JE, Tremblay LW, Boshoff HI, Barry CE 3rd, Blanchard JS.: Meropenem-clavulanate is effective against extensively drug-resistant *M. tuberculosis*. Science. 2009. 323(5918):1215-8.

29. Woldehanna S, Volmink J. Treatment of latent tuberculosis infection in HIV infected persons. *Cochrane Database Syst Rev* 2004 (1): CD000171.

30. Comstock GW, Baum C, Snider DE Jr. Isoniazid prophylaxis among Alaskan Eskimos: a fi nal report of the Bethel isoniazid studies. *Am Rev Respir Dis* 1979; **119:** 827–30.

31. Gordin FM, Cohn DL, Matts JP, Chaisson RE, O'Brien RJ. Hepatotoxicity of rifampin and pyrazinamide in the treatment of latent tuberculosis infection in HIV-infected persons: is it diff erent than in HIV-uninfected persons? *Clin Infect Dis* 2004; **39:** 561–65.

32. Jasmer RM, Saukkonen JJ, Blumberg HM, et al. Short-course rifampin and pyrazinamide compared with isoniazid for latent tuberculosis infection: a multicenter clinical trial. *Ann Intern Med* 2002; **137:** 640–47.

33. Tortajada C, Martinez-Lacasa J, Sanchez F, et al. Is the combination of pyrazinamide plus rifampicin safe for treating latent tuberculosis infection in persons not infected by the human immunodefi ciency virus? *Int J Tuberc Lung Dis* 2005; **9:** 276–81.

34. Wilkinson KA, Kon OM, Newton SM, et al. Eff ect of treatment of latent tuberculosis infection on the T cell response to *M. tuberculosis* antigens. *J Infect Dis* 2006; **193:** 354–59.

35. Munoz-Elias EJ, McKinney JD. *M. tuberculosis* isocitrate lyases 1 and 2 are jointly required for in vivo growth and virulence. *Nat Med* 2005; **11:** 638–44.

36. Trunz BB, Fine P, Dye C. Eff ect of BCG vaccination on childhood tuberculous meningitis and miliary tuberculosis worldwide: a metaanalysis and assessment of cost-eff ectiveness. *Lancet* 2006; **367:** 1173–80.

37. Young D, Dye C. The development and impact of tuberculosis vaccines. *Cell* 2006; **124:** 683–87.

38. van Rie, A., et al. Exogenous reinfection as a cause of recurrent tuberculosis after curative treatment. N. Engl. J. Med. 1999;341:1174–1179. doi: 10.1056/NEJM199910143411602.

39. Fine, P.E. The BCG story: lessons from the past and implications for the future. Rev. Infect. Dis. 1989;11(Suppl. 2):S353–S359.

40. Sterne, J.A.; Rodrigues, L.C.; Guedes, I.N. Does the efficacy of BCG decline with time since vaccination? Int. J. Tuberc. Lung Dis. 1998;2:200–207.

41. Cayabyab MJ,Hovav AH, Hsu T, Krivulka GR, LiftonMA, GorgoneDA, et al. Generation of CD8+ T-Cell responses by a recombinant nonpathogenic *M. smegmatis* vaccine vector expressinghumanimmunodeficiency virus type I Env. J Virol 2006;80(4):1645–52.

42. Kumar D, Srivastava BS, Srivastava R. Genetic rearrangements leading to disruption of heterologous gene expression in mycobacteria: an observation with Escherichia coli beta-galactosidase in *M. smegmatis* and its implication in vaccine development. Vaccine 1998;16(11–12):1212–5.

43. Harth G, Lee BY, HorwitzMA. High-level heterologous expression and secretion in rapidly growing nonpathogenic mycobacteria of four major *M. tuberculosis* extracellular proteins considered to be leading vaccine candidates and drug targets. Infect Immun 1997;65(6):2321–8.

44. EremeevW,Maiorov KB, Avdienko VG, Kondrashov SIu, Apt A. An experimental analysis of *M. smegmatis* as a possible vector for the design of a new tuberculosis vaccine. Probl Tuberk 1996;1:49–51.

45. Kuehnel MP, Goethe R, Habermann A, Mueller E, Rohde M, Griffiths G, et al. Characterization of the intracellular survival of Mycobacterium avium ssp.

paratuberculosis: phagosomal pH and fusogenicity in J774 macrophages compared with other mycobacteria. Cell Microbiol 2001;3(8):551–66.

46. Post FA, Manca C, Neyrolles O, Ryffel B, Young DB, Kaplan G. *M. tuberculosis* 19-kilodalton lipoprotein inhibits Mycobacterium smegmatisinduced cytokine production by human macrophages in vitro. Infect Immun 2001;69(3):1433–9.

47. DasGupta SK, Jain S, Kaushal D, Tyagi AK. Expression systems for study of mycobacterial gene regulation and development of recombinant BCG vaccines. Biochem Biophys Res Commun 1998;246(3):797–804.

48. Wood R, Maartens G, Lombard CJ. Risk factors for developing tuberculosis in HIV-1-infected adults from communities with a low or very high incidence of tuberculosis. *J Acquir Immune Defi c Syndr* 2000; **23:** 75–80.

49. Selwyn PA, Hartel D, Lewis VA, et al. A prospective study of the risk of tuberculosis among intravenous drug users with human immunodeficiency virus infection. *N Engl J Med* 1989; **320:** 545–50.

50. Glynn JR, Crampin AC, Yates MD, et al. The importance of recent infection with *M. tuberculosis* in an area with high HIV prevalence: a long-term molecular epidemiological study in Northern Malawi. *J Infect Dis* 2005; **192:** 480–87.

51. Marais BJ, Gie RP, Schaaf HS, Beyers N, Donald PR, Starke JR. Childhood pulmonary tuberculosis: old wisdom and new challenges. *Am J Respir Crit Care Med* 2006; **173:** 1078–90.

52. Badri M, Wilson D, Wood R. Eff ect of highly active antiretroviral therapy on incidence of tuberculosis in South Africa: a cohort study. *Lancet* 2002; **359:** 2059–64.

53. Girardi E, Sabin C, d'Arminio Monforte A, et al. Incidence of tuberculosis among HIV-infected patients receiving highly active antiretroviral therapy in europe and North America. *Clin Infect Dis* 2005; **41:** 1772–82.

54. Manosuthi W, Chottanapand S, Thongyen S, Chaovavanich A, Sungkanuparph S. Survival rate and risk factors of mortality among HIV/tuberculosis-coinfected patients with and without antiretroviral therapy. *J Acquir Immune Defi c Syndr* 2006; **43:** 42–46.

55. Lawn S, Badri M, Wood R. Tuberculosis among HIV-infected patients receiving HAART: long term incidence and risk factors in a South African cohort. *AIDS* 2005; **19:** 2109–16.

56. Currie CS, Williams BG, Cheng RC, Dye C. Tuberculosis epidemics driven by HIV: is prevention better than cure? *AIDS* 2003; **17:** 2501–08.

57. McIlleron H, Meintjes G, Burman W, Maartens G. Complications of antiretroviral therapy in patients with tuberculosis—drug interactions, toxicity and immune reconstitution infl ammatory syndrome. *J Infect Dis* 2007; **196** (suppl 1)**:** 563–75.

58. Gandhi NR, Moll A, Sturm AW, et al. Extensively drug-resistant tuberculosis as a cause of death in patients co-infected with tuberculosis and HIV in a rural area of South Africa. *Lancet* 2006; **368:** 1575–80.

59. Lawn SD, Wilkinson RJ. Extensively drug resistant tuberculosis. *BMJ* 2006; **333:** 559–60.

60. Perkins, M.D. New diagnostic tools for tuberculosis. Int. J. Tuberc. Lung Dis. 2000;4:S182–S188.

61. Perkins, M.D.; Cunningham, J. Facing the crisis: improving the diagnosis of tuberculosis in the HIV era. J. Infect. Dis. 2007;196(Suppl. 1):S15–S27.

62. Palomino, J.C. Nonconventional and new methods in the diagnosis of tuberculosis: feasibility and applicability in the field. Eur. Respir. J. 2005;26:339–350. doi: 10.1183/09031936.05.00050305.

63. Connell, T.G.; Rangaka, M.X.; Curtis, N.; Wilkinson, R.J. QuantiFERON-TB Gold: state of the art for the diagnosis of tuberculosis infection? Expert Rev. Mol. Diagn. 2006;6:663–677. doi: 10.1586/14737159.6.5.663.

64. Williams, K.J.; Duncan, K. Current strategies for identifying and validating targets for new treatment-shortening drugs for TB. Curr. Mol. Med. 2007;7:297–307. doi: 10.2174/156652407780598575.

65. Ginsberg, A.M.; Spigelman, M. Challenges in tuberculosis drug research and development. Nat. Med. 2007;13:290–294. doi: 10.1038/nm0307-290.

66. Sander, C.; McShane, H. Translational mini-review series on vaccines: Development and evaluation of improved vaccines against tuberculosis. Clin. Exp. Immunol. 2007;147:401–411.

67. Kaplan, G., et al. *M. tuberculosis* growth at the cavity surface: a microenvironment with failed immunity. Infect. Immun. 2003;71:7099–7108. doi: 10.1128/IAI.71.12.7099-7108.2003.

68. Duncan, K. Identification and validation of novel drug targets in tuberculosis. Curr. Pharm. Des. 2004;10:3185–3194. doi: 10.2174/1381612043383223.

69. Schnappinger, D., Ehrt, S., Voskuil, MI. et al.: Transcriptional adaptation of *M. tuberculosis* within macrophages: insights into the phagosomal environment. J Exp Med. 2003 Sep 1;198(5):693-704.

70. Kushner, S. R. mRNA decay in *Escherichia coli* comes of age. *J. Bacteriol.* 2002;184:4658–4665.

71. Grunberg-Manago M.: Messenger RNA stability and its role in control of gene expression in bacteria and phages. Annu Rev Genet. 1999;33:193-227.

72. Li, Z., Pandit, S., Deutscher, M. P.: RNase G (CafA protein) and RNase E are both required for the 5' maturation of 16S ribosomal RNA, EMBO J. 18 (1999) 2878-2885.

73. Ghora, B. K.; Apirion, D. Structural analysis and *in vitro* processing to p5 rRNA of a 9S RNA molecule isolated from an *rne* mutant of *E. coli. Cell.* 1978;15:1055–1066.

74. Szeberenyi, J., Roy, MK., Vaidya, HC. and Apirion D.: 7S RNA, containing 5S ribosomal RNA and the termination stem, is a specific substrate for the two RNA processing enzymes RNase III and RNase E. Biochemistry. 1984;23(13):2952-7.

75. Apirion, D., Lassar, A. B.: A conditional lethal mutant of *Escherichia coli* which affects the processing of ribosomal RNA., J. Biol. Chem. 253 (1978) 1738-1742.

76. Taraseviciene, L., Miczak, A., Apirion D.: The gene specifying RNase E (*rne*) and a gene affecting mRNA stability (*ams*), are the same gene, Mol. Microbiol. 5 (1991) 851-855.

77. Casaregola, S., Jacq, A., Laoudj, D., McGurk, G., Margarson, S., Tempete, M., Norris, V., Holland I. B.,: Cloning and analysis of the entire *Escherichia coli ams* gene. *ams* is identical to *hmp*1 and encodes a114 kDa protein that migrates as a 180 kDa protein, J. Mol. Biol. 228 (1992) 30-40.

78. Melefors, O., von Gabain A.,: Genetic studies of cleavage-initiated mRNA decay and processing of ribosomal 9S RNA show that the *Escherichia coli ams* and *rne* loci are the same, Mol. Microbiol**.** 5 (1991) 857-864.

79. Régnier, P.; Arraiano, C. M. Degradation of mRNA in bacteria: emergence of ubiquitous features. *BioEssays.* 2000;22:235–244.

80. Cohen, S. N., McDowall K. J.,: RNase E: still a wonderfully mysterious enzyme, Mol. Microbiol. 23 (1997) 1099-1106.

81. Coburn, G. A., Mackie G. A.,: Degradation of mRNA in *Escherichia coli*: an old problem with some new twists, Prog. Nucl. Acid Res. Mol. Biol. 62 (1999) 55-108.

82. Bernstein, J. A., Lin, P. H., Cohen, S. N., Lin-Chao S.,: Global analysis of *Escherichia coli* RNA degradosome function using DNA microarrays, PNAS U S A. 101 (2004) 2758-63.

83. Li, Z., Deutscher M. P.,: RNase E plays an essential role in the maturation of *Escherichia coli* tRNA precursors, RNA. 8 (2002) 97-109.

84. Lin-Chao, S., Cohen S. N.,: The rate of processing and degradation of antisense RNAI regulates the replication of ColE1-type plasmids in vivo, Cell. 65 (1991) 1233-42.

85. Lin-Chao, S., Wei, C-L., Lin Y-T.,: RNase E is required for the maturation of *ssr*A RNA and normal *ssr*A RNA peptide-tagging activity, PNAS USA 96 (1999) 12406-12411.

86. Deana, A.; Belasco, J. G. The function of RNase G in *Escherichia coli* is constrained by its amino and carboxyl termini. *Mol. Microbiol.* 2004;51:1205–1217.

87. Ow, M. C.; Perwez, T.; Kushner, S. R. RNase G of *Escherichia coli* exhibits only limited functional overlap with its essential homologue, RNase E. *Mol. Microbiol.* 2003;49:607–622.

88. Callaghan, A. J.; Marcaida, M. J.; Stead, J. A.; McDowall, K. J.; Scott, W. G.; Luisi, B. F. Structure of *Escherichia coli* RNase E catalytic domain and implications for RNA turnover. *Nature.* 2005;437:1187–1191.

89. Callaghan, A. J.; Grossmann, J. G.; Redko, Y. U. et al. Quaternary structure and catalytic activity of the *Escherichia coli* ribonuclease E amino-terminal catalytic domain. *Biochemistry.* 2003;42:13848–13855.

90. Callaghan, A. J.; Redko, Y.; Murphy, L. M.; et al. "Zn-link": a metal-sharing interface that organizes the quaternary structure and catalytic site of the endoribonuclease, RNase E. *Biochemistry.* 2005;44:4667–4675.

91. Kaberdin, V. R., Miczak, A., Jakobsen, J. S., Lin-Chao, S., McDowall, K. J., von Gabain A.,: The endoribonucleolytic N-terminal half of *Escherichia coli* RNase E is evolutionarily conserved in Synechocystis sp. and other bacteria but not the C-terminal half, which is sufficient for degradosome assembly, PNAS U S A. 95 (1998) 11637-42.

92. Leroy, A.; Vanzo, N. F.; Sousa, S.; Dreyfus, M.; Carpousis, A. J. Function in *Escherichia coli* of the non-catalytic part of RNase E: role in the degradation of ribosome-free mRNA. *Mol. Microbiol.* 2002;45:1231–1243.

93. McDowall, K. J.; Cohen, S. N. The N-terminal domain of the rne gene product has RNase E activity and is non-overlapping with the arginine-rich RNA-binding site. *J. Mol. Biol.* 1996;255:349–355.

94. Vanzo, N. F.; Li, Y. S.; Py, B.; Blum, E.; Higgins, C. F.; Raynal, L. C.; Krisch, H. M.; Carpousis, A. J. Ribonuclease E organizes the protein interactions in the *Escherichia coli* RNA degradosome. *Genes Dev.* 1998;12:2770–2781.

95. Carpousis, A. J., Van Hauwe, G., Ehretsmann, G. C., Krisch H. M.,: Copurification of *E. coli* RNase E and PNPase: evidence for a specific association between two enzymes important in RNA processing and degradation, Cell 76 (1994) 889-900.

96. Miczak, A., Kaberdin, V. R., Wei, C-L., Lin-Chao S.,: Proteins associated with RNase E in a multicomponent ribonucleolytic complex, PNAS USA 93 (1996) 3865-3869.

97. Py, B., Higgins, C.F., Krisch, H. M., Carpousis A. J.,: A DEAD-box RNA helicase in the *Escherichia coli* RNA degradosome, Nature 381 (1996) 169-172.

98. Taghbalout A, Rothfield L (2008) RNase E and RNA helicase B play central roles in the cytoskeletal organization of the RNA degradosome. J Biol Chem 283**:**13850-13855

99. Wachi, M.; Umitsuki, G.; Shimizu, M.; Takada, A.; Nagai, K. *Escherichia coli cafA* gene encodes a novel RNase, designated as RNase G, involved in processing of the 5′ end of 16S rRNA. *Biochem. Biophys. Res. Commun.* 1999;259:483–488.

100. Okada, Y.; Wachi, M.; Hirata, A.; Suzuki, K.; Nagai, K.; Matsuhashi, M. Cytoplasmic axial filaments in *Escherichia coli* cells: possible function in the mechanism of chromosome segregation and cell division. *J. Bacteriol.* 1994;176:917–922.

101. Okada, Y.; Shibata, T.; Matsuhashi, M. Possible function of the cytoplasmic axial filaments in chromosomal segregation and cellular division of *Escherichia coli*. *Sci. Prog.* 1993;77:253–264.

102. Tock, M. R.; Walsh, A. P.; Carroll, G.; McDowall, K. J. The CafA protein required for the 5′-maturation of 16 S rRNA is a 5′- end-dependent ribonuclease that has context-dependent broad sequence specificity. *J. Biol. Chem.* 2000;275:8726–8732.

103. McDowall, K. J., Hernandez, R. G., Lin. Chao, S., Cohen S. N.,: The ams-1 and rne-3071 temperature-sensitive mutations in the *ams* gene are in close proximity to each other and cause substitutions within a domain that resembles a product of the *Escherichia coli* mre locus, J. Bacteriol. 175 (1993) 4245-4249.

104. Lee, K., Cohen, S. N.: A *Streptomyces coelicolor* functional orthologue of *Escherichia coli* RNase E shows shuffling of catalytic and PNPase-binding domains, Mol. Microbiol**.** 48 (2003) 349-360.

105. Condon, C., Putzer H.,: The phylogenetic distribution of bacterial ribonucleases, Nucleic Acids Research 30 (2002) 5339-5346.

106. Carpousis, A. J. The *Escherichia coli* RNA degradosome: structure, function and relationship in other ribonucleolytic multienzyme complexes. *Biochem. Soc. Trans.* 2002;30:150–155.

107. Yang J, Jain C, Schesser K (2008) RNase E regulates the Yersinia type 3 secretion system. J Bacteriol 190:3774-3778

108. Spinelli SV, Pontel LB, García Véscovi E, Soncini FC (2008) Regulation of magnesium homeostasis in Salmonella: Mg(2+) targets the mgtA transcript for degradation by RNase E. FEMS Microbiol Lett 280:226-234

109. Russell, D. G.: *M. tuberculosis*: here today, and here tomorrow, Nature Reviews Molecular Cell Biology, 2 (2001) 569-577.

110. Briant, D. J.; Hankins, J. S.; Cook, M. A.; Mackie, G. A. The quaternary structure of RNase G from *Escherichia coli. Mol. Microbiol.* 2003;50:1381–1390.

111. Cole, S. T., Brosch, R., Parkhill, J., et al.: Deciphering the biology of *M. tuberculosis* from the complete genome sequence, Nature 393 (1998) 537-544.

112. Honer Zu Bentrup, K., Miczak, A., Swenson, DL., Russell, DG.: Characterization of activity and expression of isocitrate lyase in *Mycobacterium avium* and *M. tuberculosis,* J. Bacteriol. 181 (1999) 7161-7167.

113. Fleischmann, R. D., Alland, D., Eisen, J. A., et al.: Whole-genome comparison of *M. tuberculosis* clinical and laboratory strains, J. Bacteriol. 184 (2002) 5479-5490.

114. Tabor, S., Richardson, CC.: A bacteriophage T7 RNA polymerase/promoter system for controlled exclusive expression of specific genes, PNAS USA 82 (1985) 1074-1078.

115. Stover, CK., de la Cruz, VF., Fuerst, TR., et al.: New use of BCG for recombinant vaccines, Nature 351 (1991) 456-460.

116. Laemmli, U. K.:Cleavage of structural proteins during the assembly of the head of bacteriophage T4, Nature 227 (1970) 680-685.

117. Rosenfeld, J., Capdevielle, J., Guillemot, J. C., Ferrara P.,: In-gel digestion of proteins for internal sequence analysis after one- or two-dimensional gel electrophoresis, Anal. Biochem. 203 (1992) 173-179.

118. Altschul SF, Madden TL, Schäffer AA, Zhang J, Zhang Z, Miller W, and Lipman DJ (1997) Gapped BLAST and PSI-BLAST: a new generation of protein database search programs. Nucleic Acids Res 25**:**3389-3402

119. Gasteiger E, Hoogland C, Gattiker A, Duvaud S, Wilkins MR, Appel RD, Bairoch A (2005) Protein identification and analysis tools on the ExPASy server. In : John M. Walker (ed) The proteomics protocols handbook: Humana Press; pp 571-607

120. McDowall, K. J.; Kaberdin, V. R.; Wu, S. W.; Cohen, S. N.; Lin-Chao, S. Site-specific RNase E cleavage of oligonucleotides and inhibition by stem–loops. *Nature.* 1995;374:287–290.

121. Lin-Chao, S.; Bremer, H. Effect of the bacterial growth rate on replication control of plasmid pBR322 in *Escherichia coli. Mol. Gen. Genet.* 1986;203:143–149.

122. Pearson W. R.,, Lipman D. J.,: Improved tools for biological sequence comparision, PNAS USA**.** 85 (1988) 2444-2448.

123. Carrio, M. M., Villaverde A.,: Role of molecular chaperones in inclusion body formation, FEBS Lett**.** 537 (2003) 215-221.

124. Hartl, F. U., Martin, J., Neupert, W.: Protein folding in the cell: the role of molecular chaperones Hsp70 and Hsp60, Annu. Rev. Biophys. Biomol. Struct. 21 (1992) 293-322.

125. Kawai, S., Mori, S., Mukai, T., Suzuki, S., Yamada, T., Hashimoto, W., Murata, K.: Inorganic polyphosphate/ATP-NAD kinase of *Micrococcus flavus* and *Mycobacterium tuberculosis* H37Rv, Biochem. Biophys. Res. Commun. 276 (2000) 57-63.

126. Nishimura k, Hosaka T, Tokuyama S, Okamoto S, and Ochi K (2007) Mutations in rsmG, encoding a 16S rRNA methyltransferase, result in low-level streptomycin resistance and antibiotic overproduction in *Streptomyces coelicolor A3*(2). J Bacteriol 189**:**3876-3883

127. Afonyushkin, T.; Moll, I.; Bläsi, U.; Kaberdin, V. R. Temperature-dependent stability and translation of *Escherichia coli ompA* mRNA. *Biochem. Biophys. Res. Commun.* 2003;311:604–609.

128. Kaberdin, V. R.; Walsh, A. P.; Jakobsen, T.; McDowall, K. J.; von Gabain, A. Enhanced cleavage of RNA mediated by an interaction between substrates and the arginine-rich domain of *E. coli.* ribonuclease E. *J. Mol. Biol.* 2000;301:257–264.

129. Kaberdin, V. R.; Bizebard, T. Characterization of *Aquifex aeolicus* RNase E/G. *Biochem. Biophys. Res. Commun.* 2005;327:382–392.

130. Redko, Y.; Tock, M. R.; Adams, C. J.; Kaberdin, V. R.; Grasby, J. A.; McDowall, K. J. Determination of the catalytic parameters of the N-terminal half of. *E. coli*

ribonuclease E and the identification of critical functional groups in RNA substrates. *J. Biol. Chem.* 2003;278:44001–44008.

131. Mackie, G. A. Ribonuclease E is a 5′-end-dependent endonuclease. *Nature.* 1998;395:720–723.

132. Kaberdin, V. R. Probing the substrate specificity of *Escherichia coli* RNase E using a novel oligonucleotide-based assay. *Nucleic Acids Res.* 2003;31:4710–4716.

133. Huang, H. J.; Liao, J.; Cohen, S. N. Poly(A)- and poly(U)-specific RNA 3′ tail shortening by *E. coli* ribonuclease E. *Nature.* 1998;391:99–102.

134. Walsh, A. P.; Tock, M. R.; Mallen, M. H.; Kaberdin, V. R.; von Gabain, A.; McDowall, K. J. Cleavage of poly(A) tails on the 3′-end of RNA by ribonuclease E of *Escherichia coli*. *Nucleic Acids Res.* 2001;29:1864–1871.

135. Schnappinger, D.; Ehrt, S.; Voskuil, M. I.; et al. Transcriptional adaptation of *M. tuberculosis* within macrophages: insights into the phagosomal environment. *J. Exp. Med.* 2003;198:693–704.

136. Beste, D. J.; Peters, J.; Hooper, T.; Avignone-Rossa, C.; Bushell, M. E.; McFadden, J. Compiling a molecular inventory for *Mycobacterium bovis* BCG at two growth rates: evidence for growth rate-mediated regulation of ribosome biosynthesis and lipid metabolism. *J. Bacteriol.* 2005;187:1677–1684.

137. Archuleta, R. J.; Hoppes, P. Y.; Primm, T. P. *Mycobacterium avium* enters a state of metabolic dormancy in response to starvation. *Tuberculosis.* 2005;85:147–158.

138. Condon, C.: RNA processing and degradation in *Bacillus subtilis*, Microbiol. Mol. Biol. Rev. 67 (2003) 157-174.

139. Jiang, X.; Diwa, A.; Belasco, J. G. Regions of RNase E important for 5′-end-dependent RNA cleavage and autoregulated synthesis. *J. Bacteriol.* 2000;182:2468–2475.

140. Misra, T. K.; Apirion, D. RNase E, an RNA processing enzyme from *Escherichia coli*. *J. Biol. Chem.* 1979;254:11154–11159.

Appendix